Appendix

Appendix I

Supporting Information

Chapter 3: Results and Discussion (Part I)

Organ Targeting Drug Delivery Systems (OTDDS) of poly[(*N*-acryloyl glycine)-*co*-(*N*-acryloyl-L-phenylalanine methyl ester)] Copolymer Library and Effective treatment of Triple Negative Breast Cancer

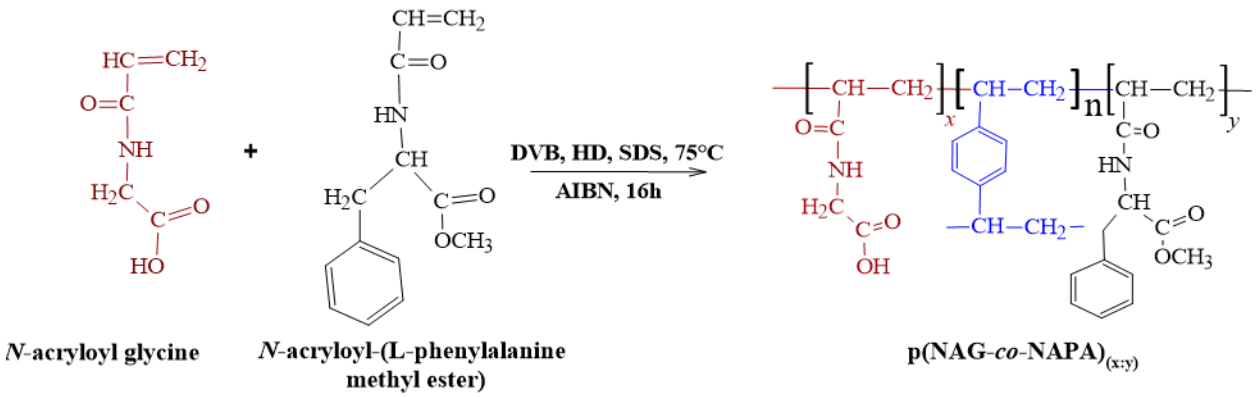

Figure S3.1.1. *Schematic for the synthesis of p(NAG-co-NAPA)$_{(x:y)}$ NPs.*

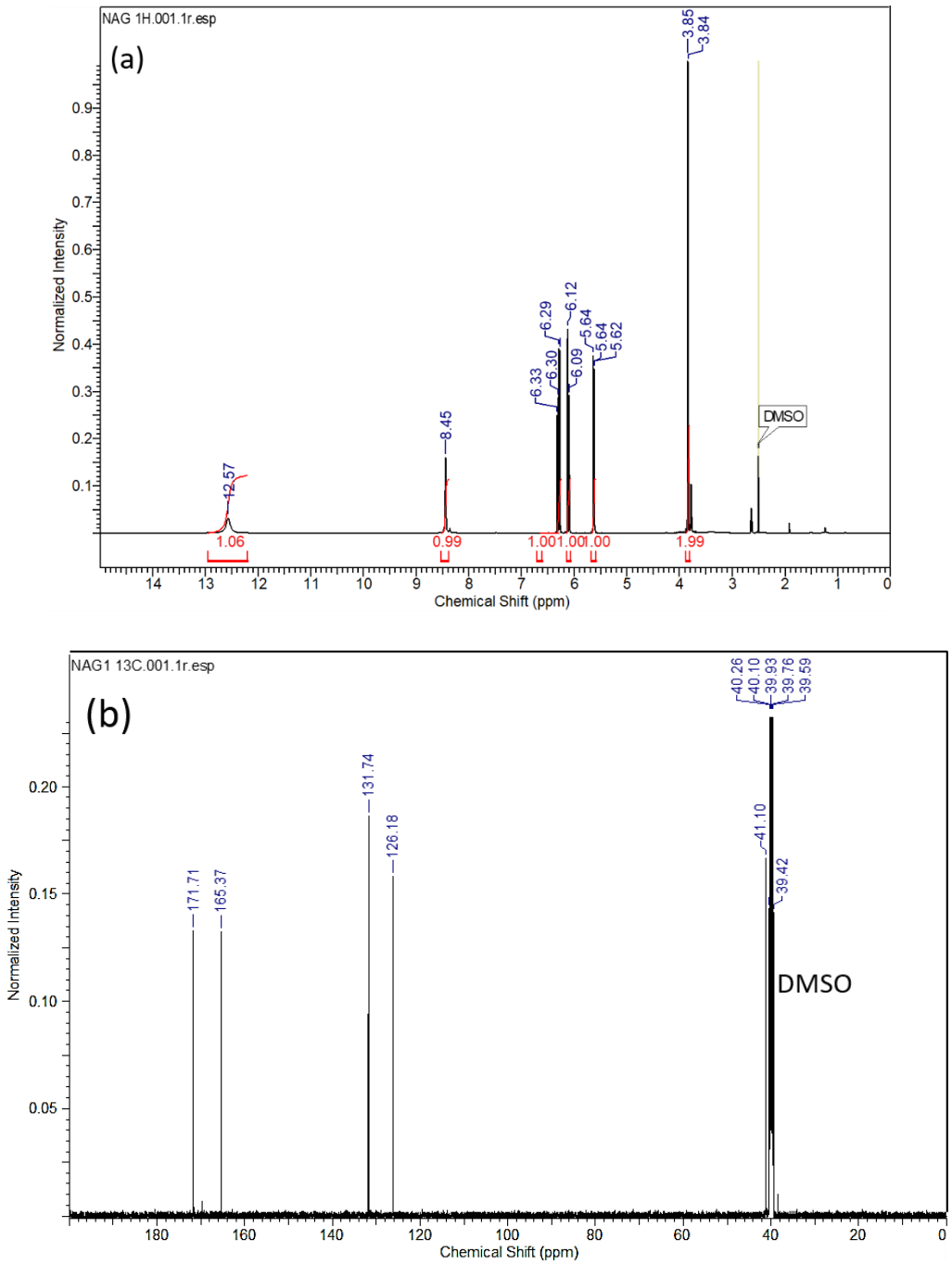

Figure S3.1.2. *(a)* ^{1}*H NMR and (b)* ^{13}*C NMR of NAG.* ^{1}*H NMR (500 MHz, DMSO-d6) δ ppm 3.84 (d, J=5.95 Hz, 2 H) 5.63 (dd, J=10.22, 2.14 Hz, 1 H) 6.11 (dd, J=17.17, 2.06 Hz, 1 H) 6.30 (dd, J=17.09, 10.22 Hz, 1 H) 8.45 (br. s., 1 H (NH)) 12.57 (br. s., 1 H (COOH));* ^{13}*C-NMR (ppm): 171.71 (-COOH), 165.37 (-C=O), 131.73 (-CH adjacent to carbonyl), and 126.18 (=CH*$_2$*).*

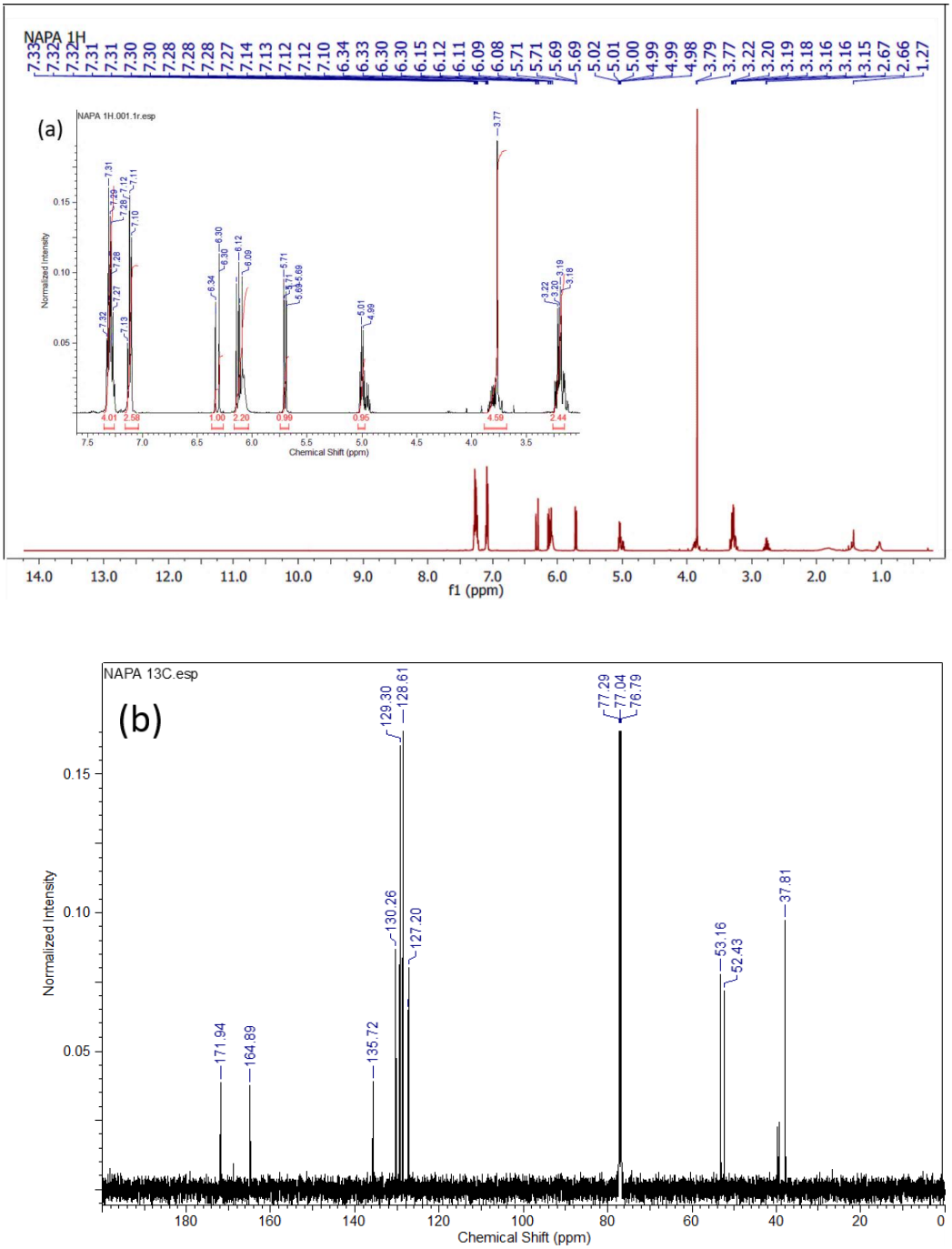

Figure S3.1.3. *(a) ^{1}H NMR and (b) ^{13}C NMR of NAPA. ^{1}H NMR (500 MHz, CHLOROFORM-d) δ ppm 3.20 (dd, J=11.14, 5.65 Hz, 3 H) 3.77 (m, 4 H) 5.00 (d, J=7.78 Hz, 1 H) 5.70 (dd, J=10.30, 1.30 Hz, 1 H) 6.04 - 6.18 (m, 2 H) 6.27 - 6.36 (m, 1 H) 7.05 - 7.16 (m, 2 H) 7.23 - 7.36 (m, 3 H); ^{13}C-NMR (ppm): 171.94 (ester), 164.89 (-C=O), 135.72 (aromatic C attached to chain), 130.26 (C adjacent to $=CH_2$), 129.30 and 128. 61 (aromatic), 127.20 ($=CH_2$), 53.16 (-CH adjacent to 2° amide), 52.43 ($-OCH_3$), and 37.81 ($-CH_2$ adjacent to aromatic ring).*

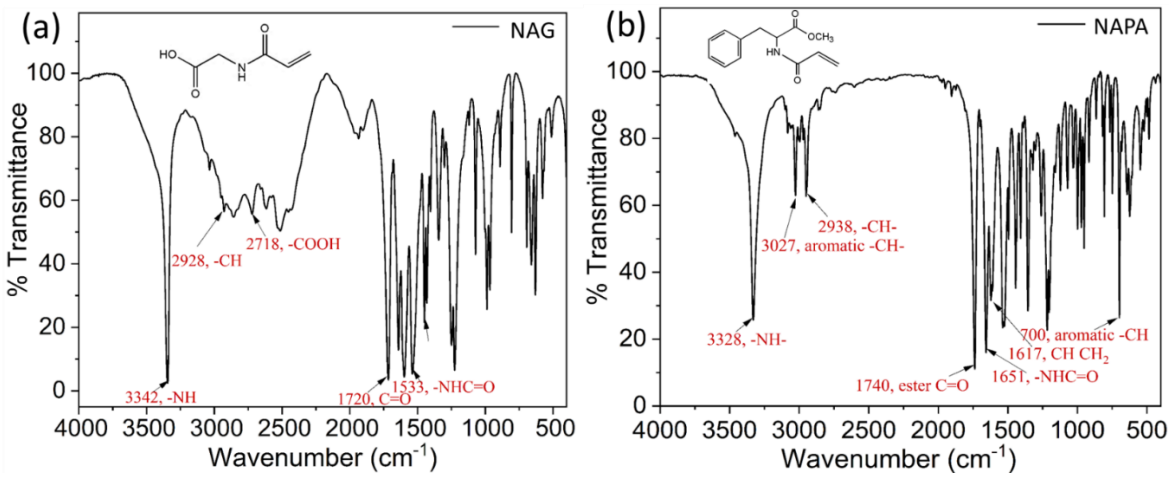

Figure S3.1.4*: FTIR spectra of (a) NAG and (b) NAPA. Respective distinct peaks corresponding to monomers are mentioned in figure (red colour). For NAG, FTIR (ATR) bands at ν (cm^{-1}) = 3342 (secondary–NH, s), 2928 (alkane, s), 2718 (-COOH), 1720 (ester C=O, s), 1533 (-CONH-, s) and for NAPA FTIR (ATR) showed characteristic bands at ν (cm^{-1}) = 3328 (secondary -NH-, s), 3027 (aromatic –CH, s) and 2938 (alkane –CH, s), 1740 (ester C=O, s), 1651 (-CONH-, s), and 700 (aromatic –CH, b).*

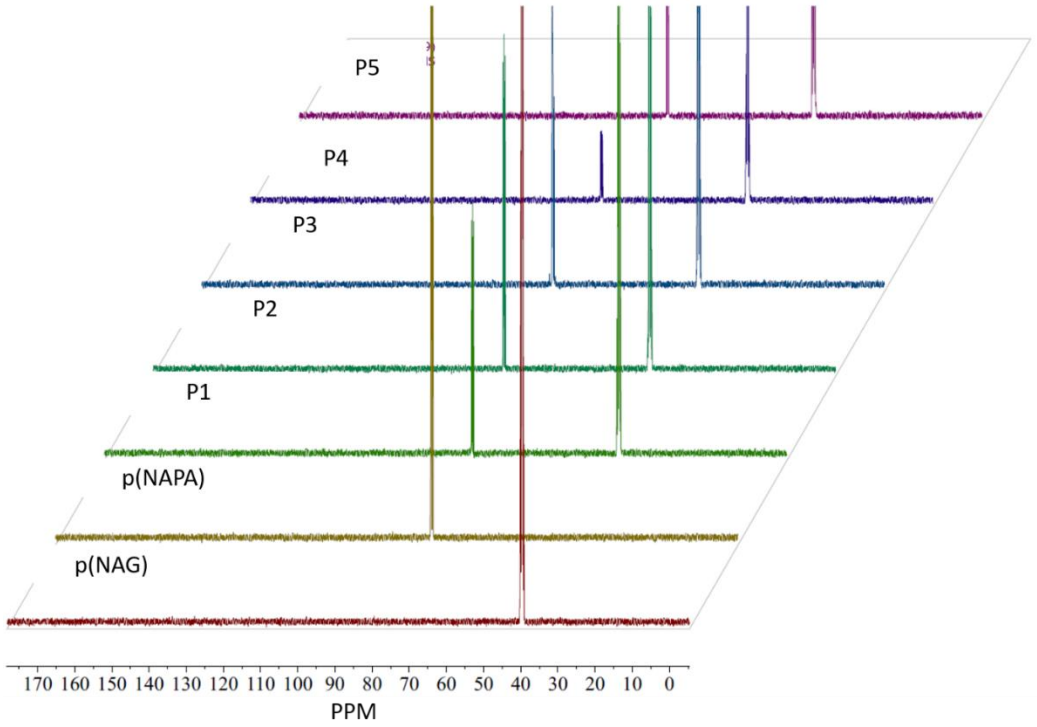

Figure S3.1.5. *Represents stacked ^{13}C NMR of p(NAG), p(NAPA), P1, P2, P3, P4, and P5. The single peak in the range of δ = 40.27 to 39.18, indicating the presence of a split 2° alkane. The at δ =70 ppm is due to solvent only.*

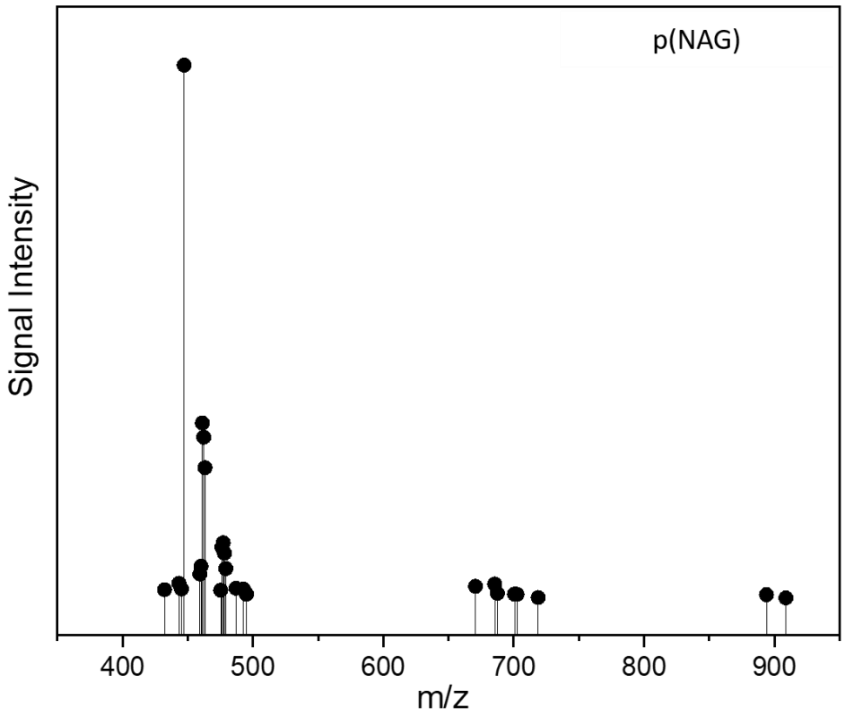

Figure S3.1.6. *MALDI-ToF spectra of p(NAG) NPs.*

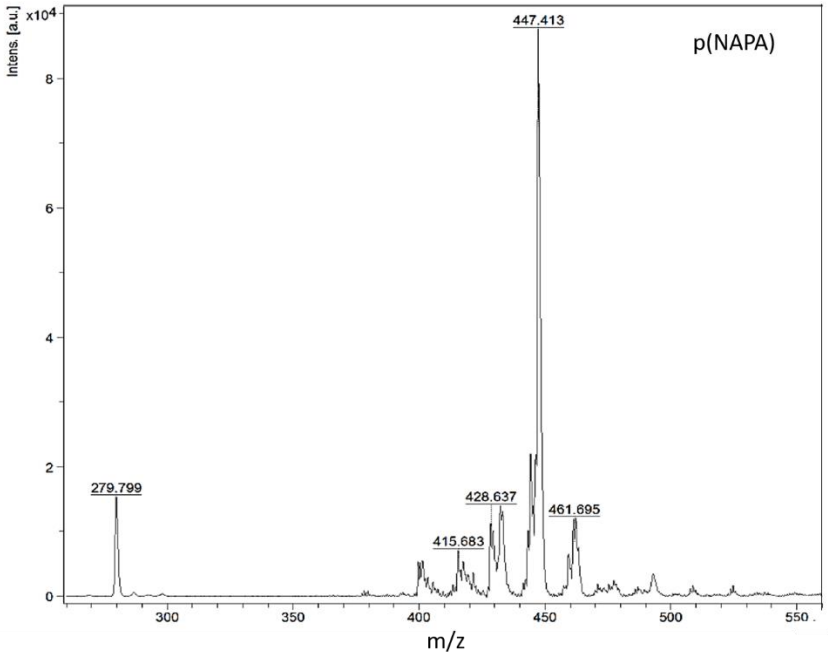

Figure S3.1.7. *MALDI-ToF spectra of p(NAPA) NPs.*

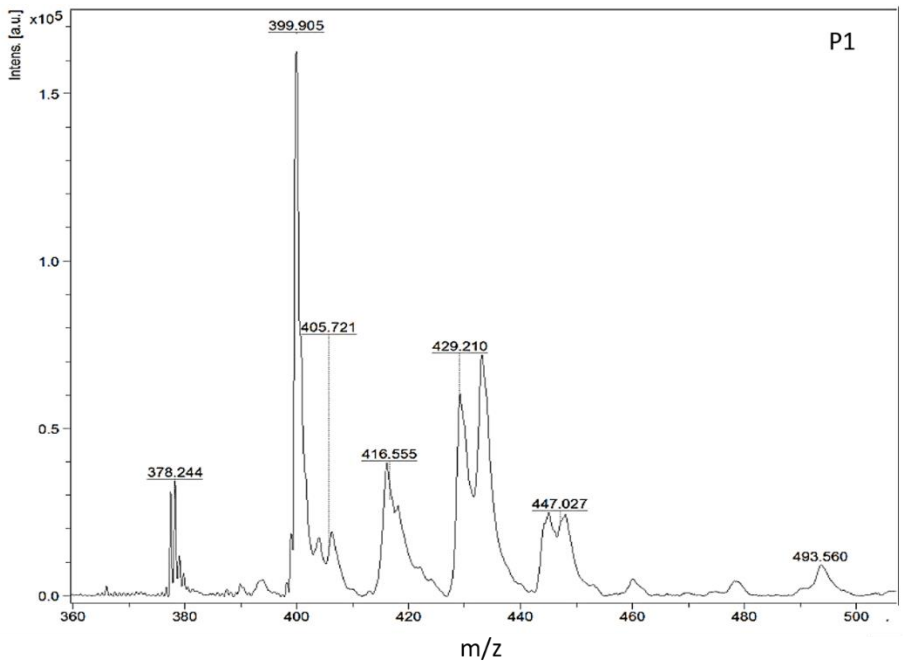

Figure S3.1.8. *MALDI-ToF spectra of P1 NPs.*

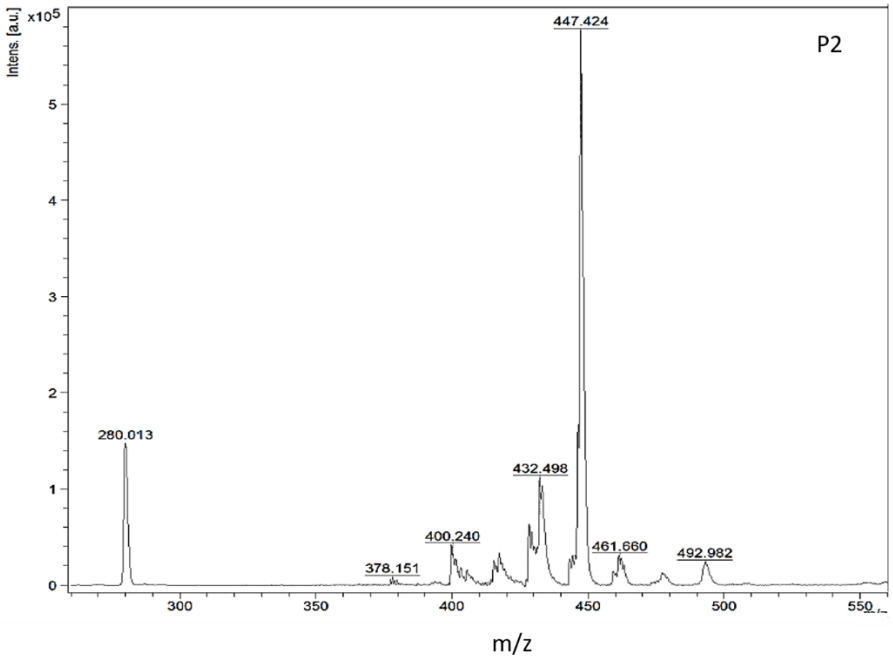

Figure S3.1.9. *MALDI-ToF spectra of P2 NPs.*

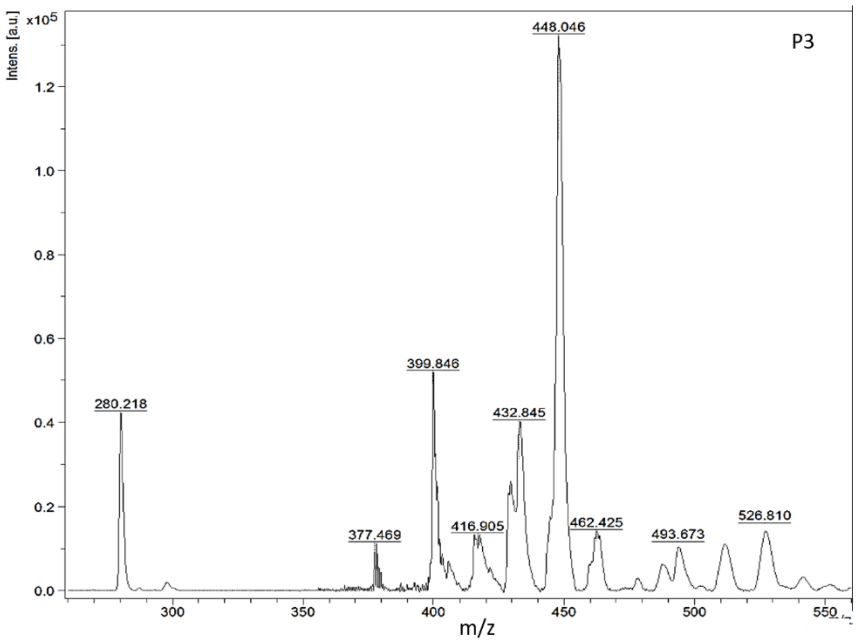

Figure S3.1.10. *MALDI-ToF spectra of P3 NPs.*

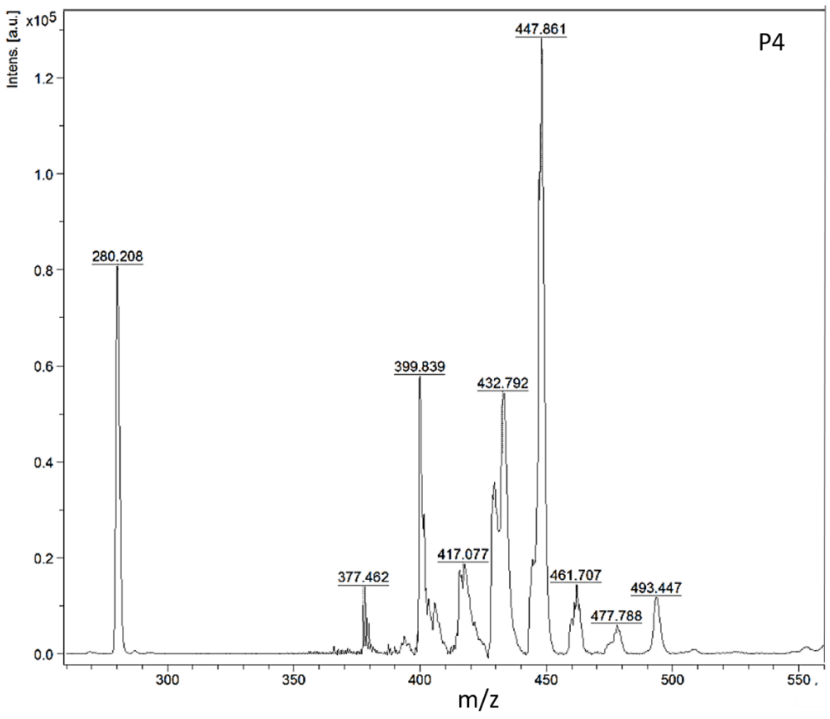

Figure S3.1.11. *MALDI-ToF spectra of P4 NPs.*

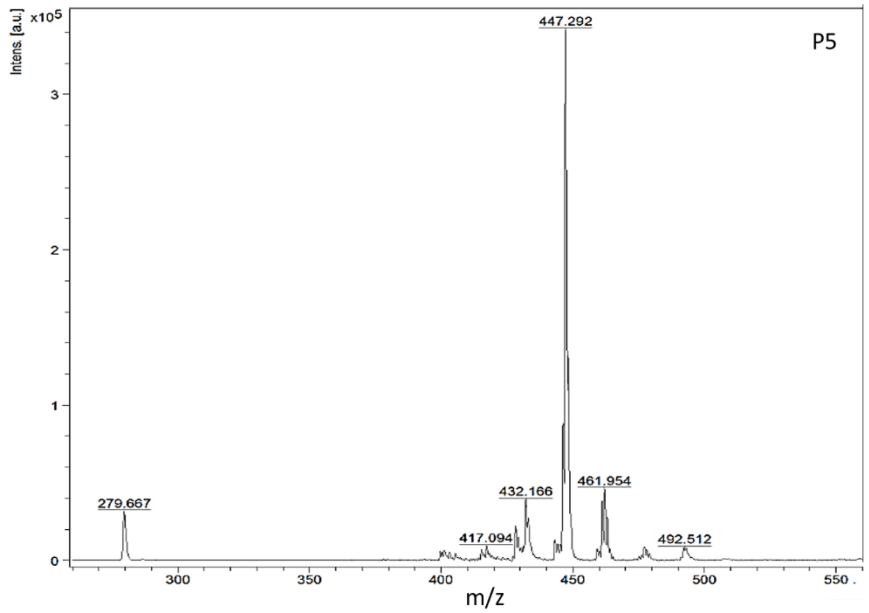

Figure S3.1.12. *MALDI-ToF spectra of P5 NPs.*

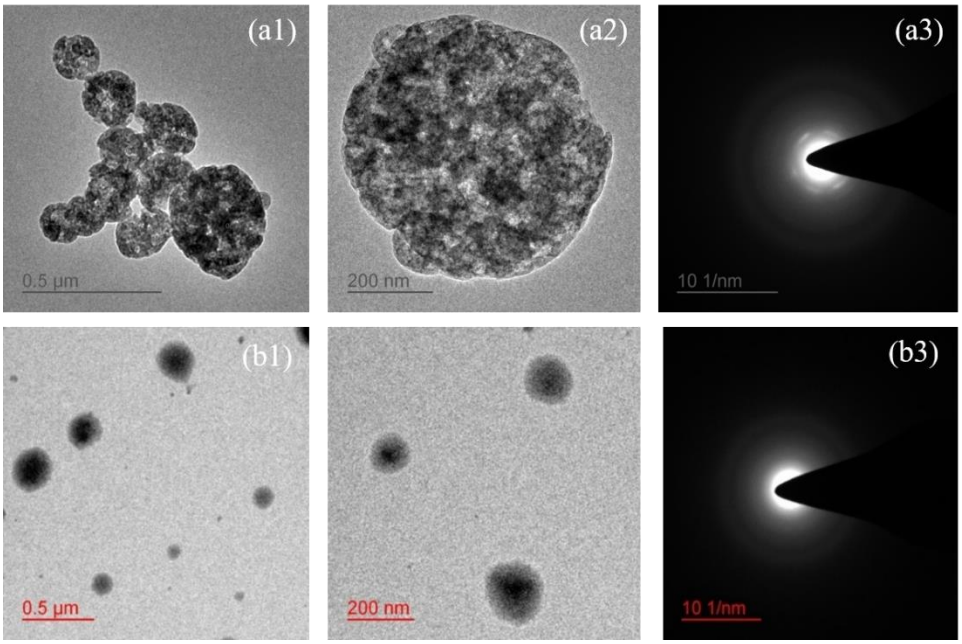

Figure S3.1.13. *HRTEM images of (a1-a3) p(NAG) and (b1-b3) p(NAPA) NPs.*

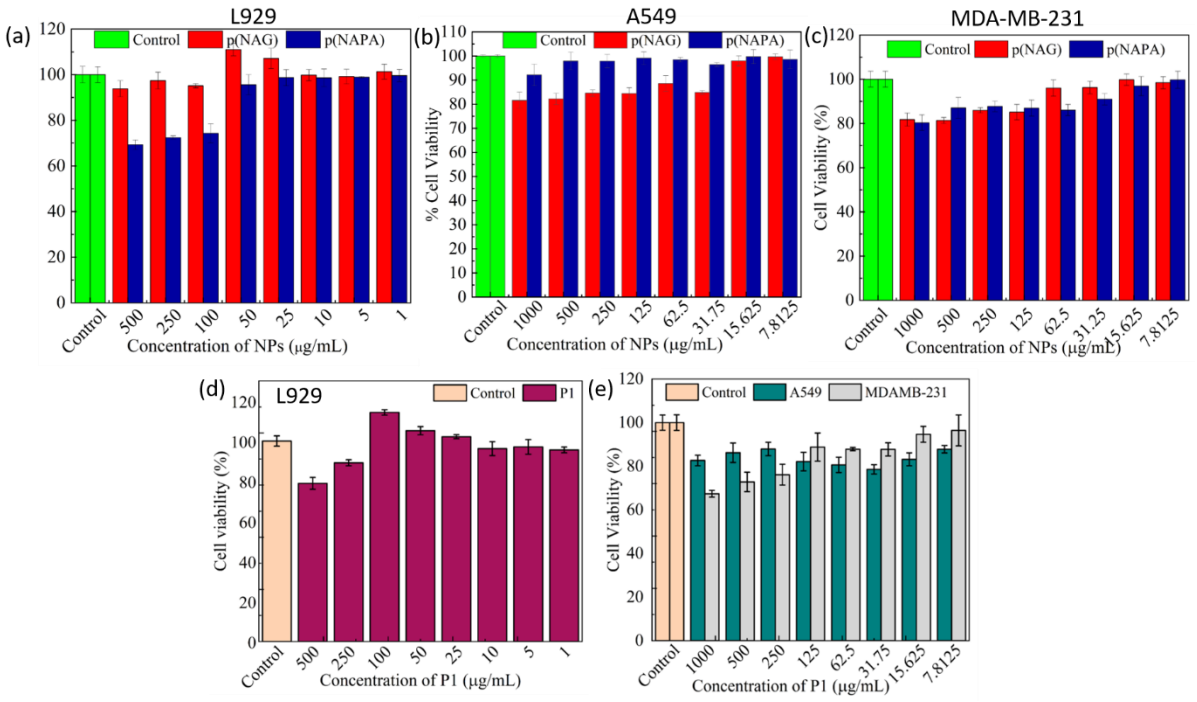

Figure S3.1.14. *Cytotoxicity study of (a-c) p(NAG) and p(NAPA) NPs against L929, A549 and MDA-MB-231 cells and (d-e) P1 NPs against L929, A549 and MDA-MB-231 cells.*

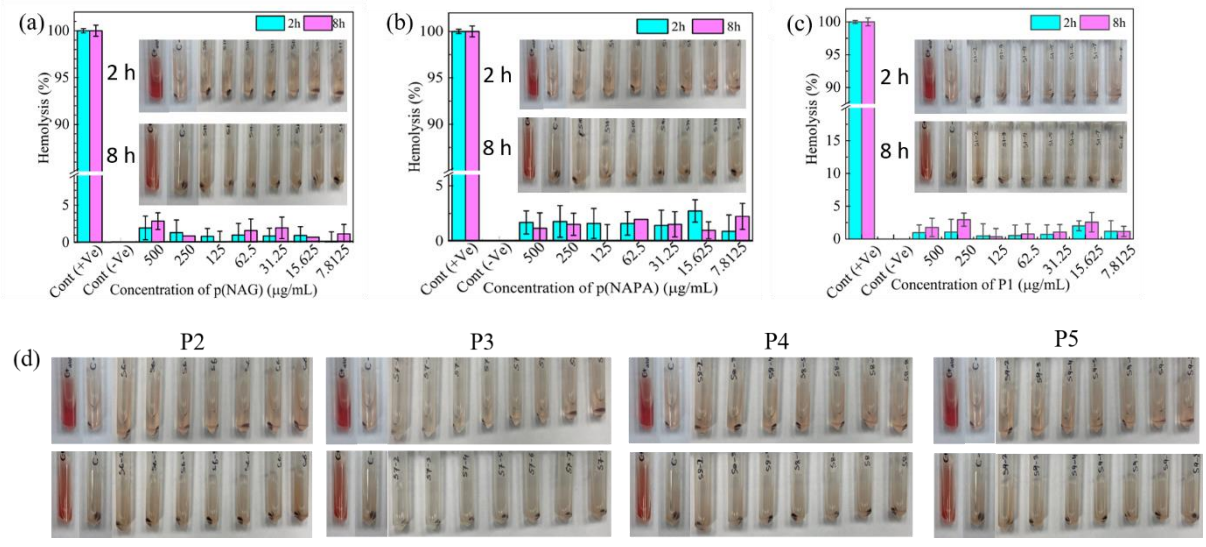

Figure S3.1.15. *Hemolysis (%) of (a) p(NAG), (b) p(NAPA), (c) P1 NPs and (d) image representation of tubes at 2 and 8 h for P2 to P5 NPs.*

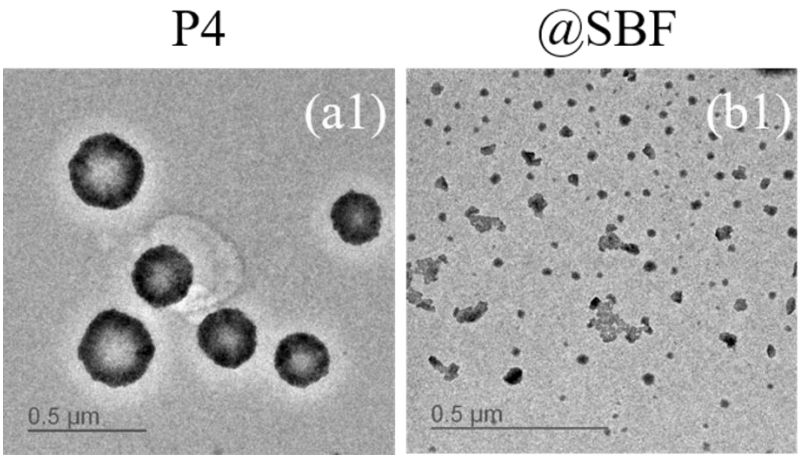

Figure S3.1.16. *HRTEM micrograph of P4 NPs incubated in SBF (pH 7.4). Results shows that after 7 days of incubation the P4 NPs degraded from 180-200 nm to fragments of 10-20 nm in size.*

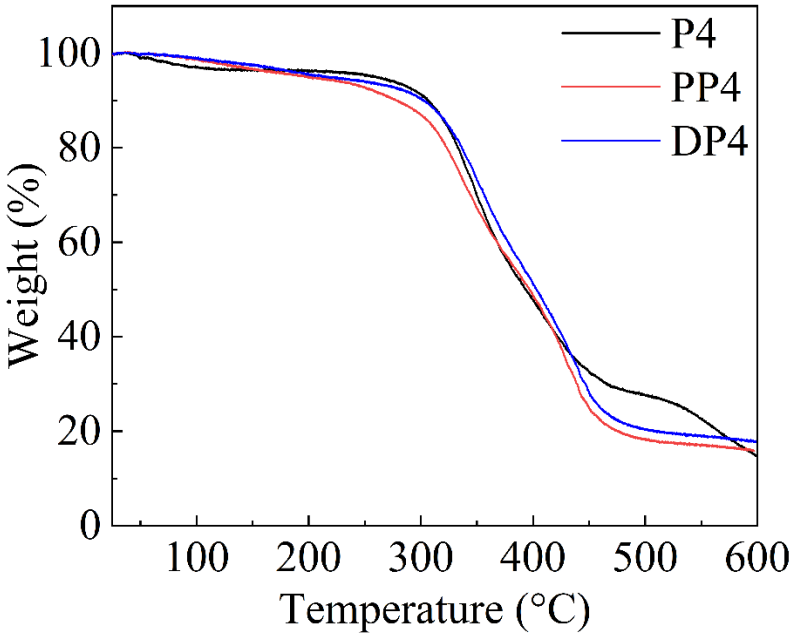

Figure S3.1.17. *TGA of P4, PP4 and DP4 NPs.*

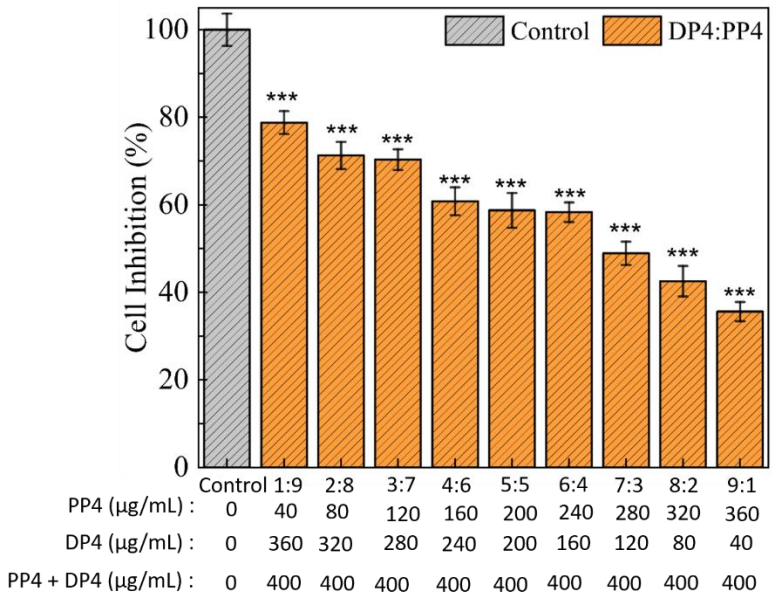

Figure S3.1.18. *Cell inhibition (%) shown by DP4:PP4 at different ratio. The final concentration is fixed to 400μg/mL.*

Table S3.1.1. List of chains, inhibitors and ions removed from protein structure before docking.

Protein Name	Removal Item
Caspase-9	Chain A, Zn^{2+}
CDK2	(4-amino-2-{[1-(methylsulfonyl)piperidin-4-yl]amino}pyrimidin-5-yl)(2,3-difluoro-6-methoxyphenyl)methanone
ER α	Chain B, N-[(1R)-3-(4-HYDROXYPHENYL)-1-METHYLPROPYL]-2-(2-PHENYL-1H-INDOL-3-YL)ACETAMIDE
BCL-2	3-nitro-n-{4-[2-(2-phenylethyl)-1,3-benzothiazol-5-yl]benzoyl}-4-{[2-(phenylsulfanyl)ethyl]amino}benzenesulfonamide
CXCR-2	Cl^-
PR	[(8s,11r,13s,14s,17r)-17-acetyl-11-[4-(dimethylamino)phenyl]-13-methyl-3-oxo-1,2,6,7,8,11,12,14,15,16-decahydrocyclopen ta[a]phenanthren-17-yl] acetate
EGFR	FLAVIN-ADENINE DINUCLEOTIDE, NADP NICOTINAMIDE-ADENINE-DINUCLEOTIDE PHOSPHATE, BICINE, caprolactone
β-tubulin	Chain A, TAXOTERE, GUANOSINE-5'-TRIPHOSPHATE, GUANOSINE-5'-DIPHOSPHATE

Bax	NA
p53	NA
C-SRC	Phosphoaminophosphonic acid-adenylate ester, l-peptide linking
HSP90	5-(5-chloro-2,4-dihydroxyphenyl)-n-ethyl-4-[4-(morpholin-4-ylmethyl)phenyl]isoxazole-3-carboxamide
P-glycoprotein	Chain B, (4S,11S,18S)-4,11,18-tri(propan-2-yl)-6,13,20-triselena-3,10,17,22,23,24-hexaazatetracyclo[17.2.1.1~5,8~.1~12,15~]tetracosa-1(21),5(24),7,12(23),14,19(22)-hexaene-2,9,16-trione
AKT1	1-(1-(4-(7-phenyl-1H-imidazo[4,5-g]quinoxalin-6-yl)benzyl)piperidin-4-yl)-1H-benzo[d]imidazol-2(3H)-one
CXCR4	(6,6-dimethyl-5,6-dihydroimidazo[2,1-b][1,3]thiazol-3-yl)methyl N,N'-dicyclohexylimidothiocarbamate, (2R)-2,3-dihydroxypropyl (9Z)-octadec-9-enoate, Glycerol
VEGF-2	Chain B
HDAC3	Chain A, Chain C, Chain D
mTOR	Chain C, Chain B, RAPAMYCIN IMMUNOSUPPRESSANT DRUG, SULFATE ION
VEGF A	Chain B, TRIETHYLENE GLYCOL, SULFATE ION
CCR5	Chain B, 4,4-difluoro-N-[(1S)-3-{(3-exo)-3-[3-methyl-5-(propan-2-yl)-4H-1,2,4-triazol-4-yl]-8-azabicyclo[3.2.1]oct-8-yl}-1-phenylpropyl]cyclohexanecarboxamide, (2R)-2,3-dihydroxypropyl (9Z)-octadec-9-enoateZn
GSK 3β	Chain B, 4-(2-methoxyphenyl)-3,7,7-trimethyl-1,6,7,8-tetrahydro-5H-pyrazolo[3,4-b]quinolin-5-one, Both L-PEPTIDE LINKING
TGF β1	Chain B
DNMT3B	Chain B, Chain C, Chain D, S-ADENOSYL-L-HOMOCYSTEINE
STAT 3	[(2-{[(5S,8S,10aR)-3-acetyl-8-({(2S)-5-amino-1-[(diphenylmethyl)amino]-1,5-dioxopentan-2-yl}carbamoyl)-6-oxodecahydropyrrolo[1,2-a][1,5]diazocin-5-yl]carbamoyl}-1H-indol-5-yl)(difluoro)methyl]phosphonic acid (non-preferred name)

Table S3.1.2. List of % of secondary structures present in different NPs of mini library.

Sample Name	α-helix (%)	β-sheet (%)	Turn	Random Coil (%)
p(NAG)	21.9	0	31.2	46.9
p(NAPA)	0	79.2	0	20.8
P1	0	0	100	0
P2	0	0	71.1	28.9
P3	0	0	77.4	22.6
P4	0	44.6	33.8	23.6
P5	0	0	55.5	44.5

Table S3.1.3. Statistical significance of Cytotoxicity study of NPs against L929 cells.

Concentration (µg/mL)	L929						
	p(NAG)	**p(NAPA)**	**P1**	**P2**	**P3**	**P4**	**P5**
500	ns	**	ns	ns	***	ns	**
250	ns	*	ns	ns	**	ns	ns
100	ns	*	ns	ns	**	ns	*
50	ns	ns	ns	ns	***	ns	ns
25	ns	ns	ns	ns	**	ns	ns
10	ns	ns	ns	ns	**	ns	ns
5	ns	ns	ns	ns	**	ns	ns
1	ns	ns	ns	ns	ns	ns	ns
ns: non-significant							

Table S3.1.4. Statistical significance of Cytotoxicity study of NPs against A549 cells.

Concentration (µg/mL)	**A549**						
	p(NAG)	**p(NAPA)**	**P1**	**P2**	**P3**	**P4**	**P5**
1000	ns	ns	ns	ns	**	*	***
500	ns	ns	ns	ns	*	***	**
250	ns	ns	ns	ns	*	ns	**
125	ns	ns	*	ns	ns	ns	ns
62.5	ns	ns	*	ns	ns	ns	ns
31.25	ns	ns	*	ns	ns	ns	ns
15.625	ns	ns	ns	ns	ns	ns	ns
7.8125	ns	ns	ns	ns	ns	ns	ns
ns: non-significant							

Table S3.1.5. Statistical significance of Cytotoxicity study of NPs against MDA-MB-231 cells.

Concentration (µg/mL)	**MDA-MB-231**						
	p(NAG)	**p(NAPA)**	**P1**	**P2**	**P3**	**P4**	**P5**
1000	***	ns	**	ns	*	ns	ns
500	***	ns	*	ns	*	ns	ns
250	ns	ns	*	ns	ns	ns	ns
125	*	ns	ns	ns	ns	ns	ns
62.5	ns	ns	ns	ns	ns	ns	ns
31.25	ns	ns	ns	ns	ns	ns	ns
15.625	ns	ns	ns	ns	ns	ns	ns
7.8125	ns	ns	ns	ns	ns	ns	ns
ns: non-significant							

Table S3.1.6. Statistical significance of Hemolysis study of NPs at 2h and 8h.

Concentration (µg/mL)	**Hemolysis**													
	p(NAG)		**p(NAPA)**		**P1**		**P2**		**P3**		**P4**		**P5**	
	2h	**8h**	**2h**	**8h**	**2h**	**8h**	**2h**	**8h**	**2h**	**8h**	**2h**	**8h**	**2h**	**8h**
500	ns	ns	ns	ns	ns	***	ns	ns	***	***	ns	ns	ns	ns
250	ns	ns	ns	ns	ns	ns	ns	*	***	**	ns	ns	ns	ns
125	ns	ns	ns	ns	ns	ns	ns	ns	ns	ns	ns	ns	ns	ns
62.5	ns	ns	ns	ns	ns	ns	ns	ns	ns	ns	ns	ns	ns	ns
31.25	ns	ns	ns	ns	ns	ns	ns	ns	ns	ns	ns	ns	ns	ns
15.625	ns	ns	ns	ns	ns	ns	ns	ns	ns	ns	ns	*	ns	*
7.8125	ns	ns	ns	ns	ns	ns	*	ns	ns	ns	ns	ns	ns	ns
ns: non-significant														

Table S3.1.7. List of proteins with their respective PDB ID considered for individual docking with ligands (piperine and DHA) and their binding energy, inhibition constant and amino acid residues.

Protein Name	PDB ID	Ligand	Binding Energy (kcal/mol)	Inhibition Constant (μM)	Amino acid residues
Bax	1f16	DHA	-6.17	30.25	Glu44, Leu125, Ala35, Leu45, Asp48, Gln32, Ala42, Pro43
Bax	1f16	Piperine	-7.92	1.57	Trp151, Leu 148,Arg147,Arg109, Asn106, Phe105, Met99, Gly103, Asn104, Asp102,Phe100
CASPASE-9	1nw9	DHA	-7.77	2	Pro336, Thr337, Leu275, Gly276, Lys280, Gly269, Phe267, Asn268, Pro338, Ile341, Ser339
CASPASE-9	1nw9	Piperine	-6.62	14.14	Pro336, Leu335, Lys280, Phe267, Asn268, Ile341, Val264, As265, Pro338, ser339, Thr337
Tubilin	1tub	DHA	-9.89	56.26	Gln43, Ile24, Glu22, Phe83, Val78, Gly84, Ile86, Ala65, Trp21, Leu44, Pro63, Ser25
Tubilin	1tub	Piperine	-10.58	0.01746	Gln8, Phe83, Ile24, Gly58, Pro63, asn59, Arg48, Tyr61, Ser25, Lys60, Glu47, Val162, Gln43, Trp21, Leu44, Val178, Ala18, gly17
p53	1ycr	DHA	-7.76	2.06	Gln59, Phe55, Leu54, Leu26, Trp23, Lys24, Met62
p53	1ycr	Piperine	-6.93	8.32	Met62, Ser20, Trp23, Lys24, Glu28, Leu26, Leu54, Lys51, Phe55, Gln59
CDK2	2fvd	DHA	-7.5	3.2	Gly16, Lys33, Asp145, Thr14, Tyr15, Gly13
CDK2	2fvd	Piperine	-9.31	0.15	Phe82, Ala31, Ala144, Leu134, Lys89, His84, Leu83
Er Alpha	2iok	DHA	-8.37	0.728	Phe445, Pro324, Glu353, Pro325, Ile326, Trp393, Arg394, Gly390, Ile386, Lys449
Er Alpha	2iok	Piperine	-8.43	0.663	Gly420, Met421, Leu428, Ile424, Arg394, Phe404, Leu391, Leu387, Glu353, Met388, His 524, Gly521

Bcl-2	2o21	DHA	-7.38	3.9	Glu149, Phe101, Phe109, Met112, Glu133, Val130, Phe150, Val131, Leu134, Ala146
Bcl-2	2o21	Piperine	-7.26	4.76	Leu94, Trp192, Phe194, Gly191, Trp141, Asn189, Leu198, Ala194, Leu182, Ile144, Ile186
C-SRC	2src	DHA	-7.34	4.13	Lys458, Leu360, Leu363, Thr456, Pro488, Cys487, Glu486, Leu358
C-SRC	2src	Piperine	-6.89	8.83	Met341, Leu393, Val281, Cys277, Gly276, Arg388, Leu273, Ala293
HSP90	2vcj	DHA	-6.07	35.74	Thr109, Gly108, Leu107, Lys58, Ile96, Gly97, Ala55, Thr184, Met98, Asn51
HSP90	2vcj	Piperine	-7.07	6.53	Thr184, Met98, Asn51, Thr109, Gly108, Gly135, Leu107, Val186, Phe138, Leu48
P-glycoprotien	3g61	DHA	-5.67	69.4	Gln326, Val732, Phe310, Ile214, Leu210, Thr314, Ile318, Tyr322, Trp311
P-glycoprotien	3g61	Piperine	-8.05	1.25	Phe263, Thr259, Val253, Val260, Leu793, Met792, Phe789, Leu254, Ala255, Phe1119, Ala256
AKT1	3o96	DHA	-8.23	0.93	Ile290, Thr211, Thr291, Asp292, Leu210, Ala212, Ser205, Leu213, Val270, Trp80, Leu264
AKT1	3o96	Piperine	-6.09	34.64	Cys296, Thr160, Lys158, Leu295, Val164, Leu156, Phe293,Gly157, Glu298, Gly159, Lys297
CXCR4	3oe6	DHA	-6.64	13.49	Ala303, Gly55, Pro299, Val59, Val62, Tyr302, Leu305
CXCR4	3oe6	Piperine	-6.92	8.51	Leu69, Gln66, Met63, leu58, val159, pro299, gly55. ala303, val62, Asp74, Tyr302
VEGFR-2	3v2a	DHA	-6.28	25.04	Gln210, Ala202, Tyr209, Glu201, Val159, Trp179, Leu151, Cys150, Cys200, Ser211
VEGFR-2	3v2a	Piperine	-5.86	50.25	Ile212, Pro149, Leu151, Cys150, Ala202, Val159, Trp179, Tyr209, Gln210, Glu201, Ser211, Tyr214

HDAC3	4a69	DHA	-6.27	25.25	Ala20, Phe144, Gly21, Pro23, Asp93, Asp92, His22, Tyr18, Pro95
HDAC3	4a69	Piperine	-8.41	0.683	Asp259, Leu266, Phe144, Tyr298, Met24, GLY296, Cys145, Gly143, Gly132, Gly295, His135, Leu133, Gln255, Asp175, Asp168, His134, His172, Asp170, Phe200, Asp93
mTOR	4drh	DHA	-6.59	14.83	Tyr113, Val186, Phe77, Gln85, Ile87
mTOR	4drh	Piperine	-7.48	3.28	Phe2108,Leu2031,Trp2101, Ser2035, Leu2097, The2098, Phe2039, Asp2102, Tyr2105, Glu2032
CxCR2	4jl7	DHA	-7.1	6.24	Arg80, Ile79, Tyr24, Phe26, Gly25, Gly23, Lys19, Asn22
CxCR2	4jl7	Piperine	-7.03	7.08	Glu43, Asn22, Gly25, Phe26, Try24, Gly23, Ile79, Arg80, His27
VEGF-A	4kzn	DHA	-5.63	74.2	Glu42, Met94, Tyr39, Ser95, Glu93, Arg82, Phe47
VEGF-A	4kzn	Piperine	-6.77	10.87	Pro40, Glu42, Tyr39, Asn75, Leu97, Glu38, Asp41
CCR5	4mbs	DHA	-6.17	29.88	Tyr37, Glu283, Tyr108, Trp86
CCR5	4mbs	Piperine	-7.45	3.45	Trp248, Tyr108, Glu283, Phe109, Trp86, Tyr37, Tyr251, Phe112
PR	4oar	DHA	-7.96	1.46	Met756, Met759, Arg766, Leu763, Phe778, Leu721, Gln725, Leu718, Gly722, Leu887, Val760, Met801
PR	4oar	Piperine	-8.18	1.01	Arg766, Leu763, Met759, Val760, Met756, Leu887, Met801, Leu797, Tyr890, Thr894, Cys891, Phe778, Leu721, Gln725
EGFR	4rg3	DHA	-8.11	1.14	Asp39, Ala142, Gly15, Val143, Phe38, Lys40, Ile14, Asn388, Ser147, Trp50, Gly46
EGFR	4rg3	Piperine	-9.24	0.169	Thr110, val112, Glu111, Gly46, Thr47, Gly144, Phe18, Ile441, Gly19, Ala142, Asp39, Gly15, Lys40, Phe38, Ile14
GSK3 Beta	5hlp	DHA	-7.05	6.84	Pro136, Val135, Tyr134, Ala83, Leu132, Asp133, Cys199, Leu188, Thr138

GSK3 Beta	5hlp	Piperine	-5.39	111.69	Gln99,Lys94, Asn95, Asp90, Phe93, Gln89, Val126, Tyr177, Leu98, Arg102
TGF-Beta1	5vqp	DHA	-5.71	65.53	Leu51, Val48, Thr55, Tyr52, Lys77, Glu78, Val79
TGF-Beta1	5vqp	Piperine	-8.04	1.28	His222, Arg215, Ile221, Tyr92, Val85, Tyr103, Ile91, Phe105, Asn89, Thr87, Glu86, His88
DNMT3B	6kdl	DHA	-7.83	1.83	Arg832, Cys651, Glu697, Ser833, Trp834, Asp582, Gly583, Phe581, Glu605, Pro650, Gly648, Ser649
DNMT3B	6kdl	Piperine	-9.26	0.162	Arg832, Ser604, Glu605, Val606, Gly648, Val628, Phe581, Asp627, Trp834, Leu671, Ser833, Asp582
STAT3	6njs	DHA	-6.82	9.98	Asp334, Lys573, Asp570, Ile569, Lys574, Arg335, Met331, His332, Pro333
STAT3	6njs	Piperine	-6.15	30.96	Arg609, Pro639, Thr620, Glu638, Ser636, Tyr657, Val637, Glu612, Ser613, Ser611

Table S3.1.8. Docking results of 8 selected proteins with combination of ligands (piperine followed by DHA)

Sr. No.	**PDB ID**	**Combination type (Piperine_DHA)**				**Paclitaxel**		
		Binding Energy (kcal/mol)	**Inhibition constant (µM)**	**Amino acid residues**		**Binding Energy (kcal/mol)**	**Inhibition constant (µM)**	**Amino acid residues**
				Piperine	DHA			
1	1tub	-7.87	1.69	Gln8, Phe83, Ile24, Gly58, Asn59, Pro63, Arg48, Tyr61, Ser25, Lys60, Glu47, Val62, Gln43, Trp21, Leu44, Val78, Ala18, Gly17	Leu371, Ser232, His229, Phe272, Leu230, Ala233, Leu217, Leu275, Thr276, Pro274	-6.24	26.47	Thr314, Pro261, Val260, Phe262, Pro263, Arg264, Glu431, Tyr435, Trp346, Ile347

2	4jl7	-6.58	15	Asn22, His27, Gly25, DHA, Ile79, Phe26, Arg80, Gly23, Tyr24, Glu43	His27, PIP, Phe26, Arg80, Leu28, Val176, His72	-4.81	300.48	Phe26, Gly25, Arg80, Ile79, Val76, His72, Gis29, Gly30, His27, Arg40, Leu28, Gly23, Tyr24
3	1nw9	-7.09	6.32	Pro336, Leu335, Lys280, Phe267, Asn268, Ile341, Val264, Asn265, Pro338, Ser339, Thr337	Lys414, Arg146, Thr415, Phe413, Try153, Phe412, Leu155, Ser156	-6.83	9.89	Thr347, Gly395, phe348, Ile396, Pro349, Trp354, phe351, Gly350, Arg355, Lys398, arg178, Leu177, Gly176, His237, Cys287, Gly288
4	2o21	-7.47	3.37	Leu94, trp192, Phe195, Gly191, Trp141, Asn189, Leu198, Ala194, Leu182, Ile144, Ile186	Ala146, Glu149, Leu134, Phe150, Val130, Val131, Glu133, Met112, Phe109, Phe101	-5.3	129.56	Arg143, tyr105, Gly142, tyr199, Ala97, Gln96, Thr93, Pro201, Asp100, Val145, Phe101, Arg104
5	4oar	-7.15	5.69	Gln725, Phe778, Leu721, Met759, DHA, Thr894, Leu797, Leu887, Cys891, Tyr890, Met801, Val760, Met756, Arg766, Leu763	PIP, Trp755, Gly722, leu726, Met759, Glu723, Asn719, Leu718	-2.63	11780	Gln752, Ile751, Trp755, Gln916, Asn719, Ala915, Phe895, Leu726, Val730
6	2iok	-8.22	0.94	Glu353, Met421, Gly420, Gly521, His524, Arg394, Leu391, Leu387, Met388, Phe404, Ile424, Leu428	Glu353, Leu327, Pro325, Ile326, try393, Arg394, Phe445, Gly390, lys449, Pro324, Ile386	-4.29	716.79	Leu536, Glu380, Ala350, Trp383, Leu354, Thr347, Asp351, Val355, Leu539, Pro535, Tyr526, Lys529, Met528, Leu525
7	4rg3	-7.44	3.5	Thr110, Val112, Glu111, Gly46, Thr47, Gly144, Phe18, Ile441, Gly19, Ala142,	Thr60, tyr65, Phe248, Thr47, ser58, Asp59,	-1.84	44580	His166, Trp50, Lys40, Arg52, Asp42, Tyr49, Glu172, Pro171,

				Asp39, gly15, Lys40, Phe38, Ile14	Leu57, Arg329, trp48			Trp170, Ala169, Thr164, phe151
8	2fvd	-7.89	1.64	Ala31, Ala144, Leu134, Lys89, His84, Leu83, Phe82	Lys33, Gly16, Asp145, Gly13, Tyr15, Thr14	-4.76	326.45	Ile10, Glu12, Gly11, Gln131, Asn132, Glu162, Lys88, Asp86, Lys89, Asp92

Table S3.1.9. Docking results of 8 selected proteins with combination of ligands (DHA followed by piperine)

Sr. No.	PDB ID	Combination type (DHA_piperine)				Paclitaxel		
		Binding Energy (kcal/mol)	Inhibition constant (µM)	Amino acid residues		Binding Energy (kcal/mol)	Inhibition constant (µM)	Amino acid residues
				DHA	Piperine			
1	1tub	14.53	--	Pro63, Leu44, Ser25, Ile24, Gln43, Glu22, Trp21, Val78, Gly84, Phe83, Ile86, Ala65	Asn206, Leu209, Ile16, Val231, Gln8, Phe20, Gln136, Leu137, His6, Trp21, Ile7, Met235, Phe169, Thr138, Ile204, Val171, Ser170	-6.24	26.47	Thr314, Pro261, Val260, Phe262, Pro263, Arg264, Glu431, Tyr435, Trp346, Ile347
2	4jl7	-7.35	4.12	Ile79, Arg80, PIP, Tyr24, Gly25, Asn22, Phe26, Gly23, Lys19	Val76, DHA, His27, Gly25, Glu43, Asn22, Phe26, Leu28	-4.81	300.48	Phe26, Gly25, Arg80, Ile79, Val76, His72, Gis29, Gly30, His27, Arg40, Leu28, Gly23, Tyr24
3	1nw9	-6.86	9.39	Gly269, Lys280, Asn268, Ile341, Pro338, Phe267, Ser339, Thr337, Pro336, Gly276, Leu275	Cys287, Phe351, Pro357, Thr179, Arg178, Thr181, Ser183, Arg180, Asp186, Ser361	-6.83	9.89	Thr347, Gly395, phe348, Ile396, Pro349, Trp354, phe351, Gly350, Arg355, Lys398, arg178, Leu177, Gly176, His237, Cys287, Gly288

4	2o21	-7.12	6.04	Phe101, Leu134, Glu149, Ala146, Phe150, Val131, Val130, Met112, Glu133, Phe109	Tyr26, Glu27, Asp29, Ser164, Pro165, Trp28, Asp168	-5.3	129.56	Arg143, tyr105, Gly142, tyr199, Ala97, Gln96, Thr93, Pro201, Asp100, Val145, Phe101, Arg104
5	4oar	-7.91	1.59	Met756, Met801, Leu887, Val760, Leu718, Leu763, Gly722, PIP, Gln725, Leu721, Arg766, Phe778, Met759	Phe794, Met801, Leu797, Leu718, Leu726, Gly722, Asn719, DHA, Trp755, Phe778, Met759, Glu723	-2.63	11780	Gln752, Ile751, Trp755, Gln916, Asn719, Ala915, Phe895, Leu726, Val730
6	2iok	-8.09	1.18	Glu353, Pro325, Ile326, Gly390, Trp393, Phe445, lys449, Ile386, Pro324, Arg394	Glu353, Leu391, leu387, Leu346, Met421, Met343, Val418, Met528, His524, Glu419, Gly420, Ile424, Leu349, Phe404, Ala350, Arg394	-4.29	716.79	Leu536, Glu380, Ala350, Trp383, Leu354, Thr347, Asp351, Val355, Leu539, Pro535, Tyr526, Lys529, Met528, Leu525
7	4rg3	-9.24	0.167	Lys40, Ile14, Gly15, Ala142, Phe38, Asp39, Val143, Gly46, Ser147, Trp50, Asn388	Leu437, Thr435, Phe434, Phe507, Leu145, Trp492, Leu146, Phe382, Gly381, Thr189, Gly187, Ser188, Arg329, Phe279	-1.84	44580	His166, Trp50, Lys40, Arg52, Asp42, Tyr49, Glu172, Pro171, Trp170, Ala169, Thr164, phe151
8	2fvd	-9.19	0.183	Thr14, Asp145, Tyr15, Gly16, Lys33, Gly13,	Val64, Ala31, Leu83, Phe82, Leu134, Lys89, Gln85, His84, Val18, Glu81, Phe80	-4.76	326.45	Ile10, Glu12, Gly11, Gln131, Asn132, Glu162, Lys88, Asp86, Lys89, Asp92

Appendix II

Supporting Information

Chapter 3: Results and Discussion (Part II)

Co-delivery of Dihydroartemisinin and Piperine by Folate decorated poly[(*N*-acryloyl glycine)$_1$-*co*-(*N*-acryloyl-L-phenylalanine methyl ester)$_4$] copolymer for Triple Negative Breast Cancer Treatment

Before using these equations to fit any of the equations, equations should be converted in the form of the fraction of drugs released with time to get comparable fitting values for each model by using the following method:

1. **Zero Order Model**

   This model describes the steady-state drug release over time, independent of the amount of drug remaining in the dosing solution. If you plot the cumulative amount of time released, a straight line will emerge.

   Equation for Zero Order Release is :

   $$Q_t = Q_0 + k_0 \times t \ldots\ldots\ldots S3.2.1$$

   Where Q_t means the amount of drug dissolved at time t, Q_0 is the initial dissolved drug quantity if zero and k_0 is the order of zero.

   $$Q_t = k_0 \times t \ldots\ldots\ldots\ldots\ldots S3.2.2$$

For the equation to be represented as the fraction of drug release per unit of time t, we take as the fraction of drug release (F) of the time t. where, $M_t \; and \; M_\infty$ are amount released at time t and amount to be released respectively.

$$\frac{M_t}{M_\infty} = \frac{k_0}{M_\infty} \times t \; \ldots\ldots S3.2.3$$

$$F = K_0 \times t \; \ldots\ldots\ldots\ldots S3.2.4$$

Here, F is Fraction of Drug released at time t and K_0 is new zero order constant.

Assumptions:

- The system does not disaggregate.
- The drug release surface area remains constant.
- The concentration gradient remains constant.

Controlled geometry or saturated release mechanism may contribute to the likely constant drug release in the drug delivery system, if the release curve shows a nearly linear increase in the fraction of drug released over time for large fractions of releases. This is often required to achieve a sustained pharmacological effect and maintain a stable level of the drug in the body.

2. **First Order Model:**

This model describes a release rate that is **proportional to the amount of drug remaining** in the dosage form. The release rate decreases over time. When log of the remaining drug is plotted versus time, it yields a straight line.

Equation:

$$\frac{dC}{dt} = -k \times C \; \ldots\ldots S3.2.5$$

Upon integration we get,

$$\log C = \log C_0 - \frac{K_1 \times t}{2.303} \ldots\ldots\ldots\ldots S3.2.6$$

Where, C stands for Concentration of drug at time t, C_0 initial Concentration of drug and K_1 is first order constant. In terms of amount released we can write this Equation as $Q_t = Q_0(1 - e^{-K_1 t})$ where Q_0 is total amount of drug. To express this in fraction released $\frac{M_t}{M_\infty}$, where M_∞ is Q_0

$$F = \frac{M_t}{M_\infty} = 1 - e^{(-K_1 \times t)} \dots\dots\dots\dots\dots\dots\dots S3.2.7$$

Here, F is Fraction of Drug released at time t and K_1 is first order rate constant.

Assumptions:

- The drug release is driven by the amount of drug available in the system
- It can describe dissolution of water-soluble drugs from porous matrices

If release curve shows a rapid initial release followed by a progressively slower release that approaches a plateau, it suggests that the release is likely governed by the concentration of the drug within the delivery system. This is common for systems where the drug is readily available and the release is not significantly controlled by barriers or matrix properties.

3. **Higuchi Model:**

This model describes the release of drugs from an insoluble matrix as a function of the square root of time. It is based on Fickian diffusion principles.

Equation for Higuchi Model release is :

$$M_t = k_H \times \sqrt{t} \dots\dots\dots\dots\dots\dots\dots S3.2.8$$

Where, M_t is amount of drug release at time t and k_H is the Higuchi dissolution constant. In order to express in terms of Fraction of drug released (F).

$$\frac{M_t}{M_\infty} = \frac{k_H}{M_\infty} \times \sqrt{t} \dots\dots\dots\dots\dots S3.2.9$$

$$F = K_H \times \sqrt{t} \dots\dots\dots\dots\dots S3.2.10$$

Here, F is Fraction of Drug released at time t and K_H is a new Higuchi dissolution constant.

Assumptions:

- Initial drug concentration in the matrix is much higher than drug solubility
- Drug diffusion takes place only in one dimension (edge effects are negligible).
- Drug particles are much smaller than system thickness.
- Matrix swelling and dissolution are negligible.
- Drug diffusivity is constant.
- Perfect sink conditions are always attained in the release environment.

If plot of fraction released versus square root of time is linear, it suggests that the drug release from your system is primarily controlled by **diffusion through a non-swelling matrix**. This is common for matrix tablets with poorly soluble drugs.

4. **Korsmeyer-Peppas Model:**

This is a semi-empirical model used to describe drug release from polymeric systems. The value of the release exponent 'n' provides insights into the drug release mechanism.

Equation for Korsmeyer-Peppas Model release is:

$$\frac{M_t}{M_\infty} = K_{KP} \times t^n \dots\dots\dots\dots S3.2.11$$

Where, $\frac{M_t}{M_\infty}$ is fraction of drug release at time t, K_{KP} is the release rate constant and n is the release exponent. This equation is typically applied to the first 60% of drug release.

Assumptions:

- Valid for the first 60% of drug release.
- Drug release mechanism is consistent over this initial period.

The value of 'n' from the Korsmeyer-Peppas model can indicate the release mechanism:

For thin films (or slabs):

- n ≈ 0.5: Indicates Fickian diffusion (drug movement driven by the concentration gradient)
- 0.5 < n < 1.0: Indicates non-Fickian (anomalous) transport (drug release governed by both diffusion and polymer relaxation).
- n ≈ 1.0: Indicates Case-II transport (drug release controlled by polymer relaxation/swelling). Case II transport is characterized by a release rate independent of time, leading to zero-order release.

For cylindrical matrices:

n ≈ 0.45: Indicates Fickian diffusion.

0.45 < n < 0.89: Indicates non-Fickian transport.

n ≈ 0.89: Indicates Case II transport.

n > 0.89: Indicates super Case II transport (suggests a release rate that **increases with time**)

For spheres:

n<0.43: Indicates Fickian diffusion with diffusion-controlled release

n = 0.43: Indicates Fickian diffusion.

0.43 < n < 0.85: Indicates anomalous transport.

n = 0.85: Indicates Case-II transport.

5. **Hixson-Crowell Model:**

This model describes drug release from systems where there is a **change in surface area and diameter of particles or tablets** during the dissolution process, maintaining geometric similarity. It is based on the cube root law.

Equation for Hixson-Crowell Model:

$$W_0^{\frac{1}{3}} - W_t^{\frac{1}{3}} = k \times t \ldots\ldots\ldots\ldots\ldots S3.2.12$$

Where, W_0 and W_t are initial amount of drug and amount of drug remaining at time t and k is a constant. To express in terms of amount of drug released relative to the initial amount we get,

$M_{\infty}^{\frac{1}{3}} - (M_{\infty} - M_t)^{\frac{1}{3}} = k \times t \ldots\ldots\ldots S3.2.13$ (Since, $M_t = W_0 - W_t$ and $M_{\infty} = W_0$)

To express in terms of fraction of drug released:

$$1 - (1 - F)^{\frac{1}{3}} = \frac{k}{M_{\infty}^{\frac{1}{3}}} \times t \ldots\ldots\ldots\ldots S3.2.14$$

$$1 - (1 - F)^{\frac{1}{3}} = K_{HC} \times t \ldots\ldots\ldots S3.2.15$$

Here, F is Fraction of Drug released at time t and K_{HC} is a new Hixson-Crowell constant.

Assumptions:

- Drug powder has uniform sized particles.
- The shape of the dissolving particles remains geometrically similar

If a plot of $1 - (1 - F)^{\frac{1}{3}}$ versus time is linear, it suggests that the release rate is controlled by the progressive **reduction in the size and surface area** of the drug-containing matrix. This is relevant for dissolving tablets or particles with a constant shape factor.

6. <u>Weibull Model:</u>

This is an **empirical model** that can describe various types of drug release profiles, including those with different shapes (e.g., exponential, sigmoidal). The shape parameter 'b' can provide insights into the release mechanism.

Equation for Weibull Model is given by:

$$M_t = M_{\infty}(1 - e^{-(t-T)^{\frac{b}{a}}} \ldots\ldots\ldots S3.2.16$$

In terms of fraction of drug released assuming no lag time, T=0

$$F = \frac{M_t}{M_{\infty}} = 1 - e^{-t^{\frac{b}{a}}} \ldots\ldots\ldots\text{S3.2.17}$$

M_t and M_∞ are amount of drug released at time t and total amount of drug being released, F is fraction of drug released, T accounts for a lag time in the dissolution process. Whereas, “a” is a scale parameter that describes the time dependence and is related to the time for 63.2% drug release and “b” is a shape parameter that describes the shape of the dissolution curve progression and provide insights into the release mechanism.

Assumptions:

This model is flexible and can fit a wide range of release profiles without strict mechanistic assumptions

The Weibull model is often used to compare dissolution profiles. The value of 'b' can give an indication of the release mechanism:

- **b = 1:** Corresponds to first-order release (exponential).
- **b > 1:** Indicates a more complex release profile, often with an initial steep increase.
- **b < 1:** Suggests a slower release, possibly due to diffusion-controlled mechanisms.

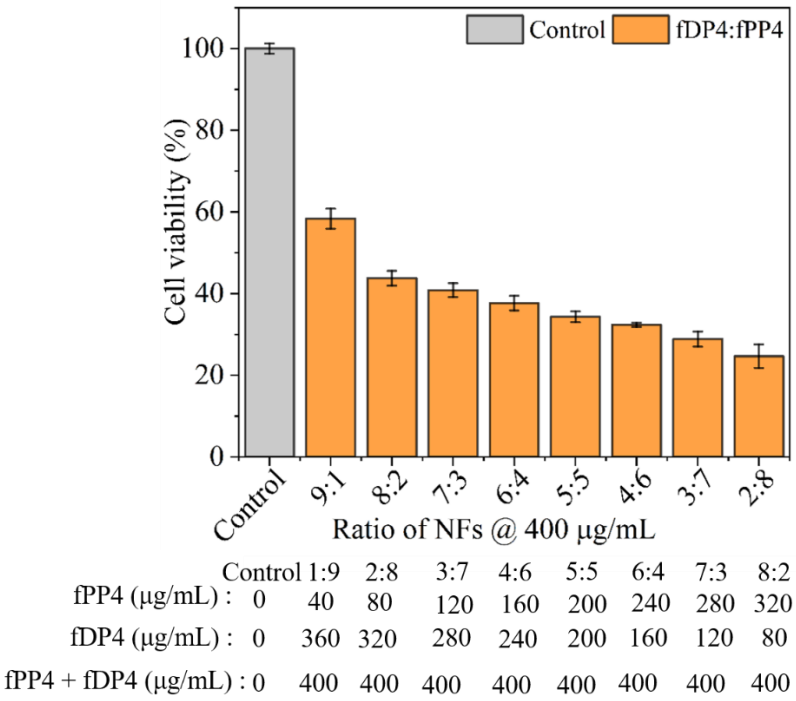

Figure S3.2.1: *Cell inhibition (%) shown by DP4:PP4 at different ratio. The final concentration is fixed to 400µg/mL.*

Table S3.2.1: R^2 values for different mathematical models used to study the drug release kinetics.

Sample Name	Zero Order	First Order	Hixson-Crowell	Weibull
fDP4 (pH 6.8)	0.16668	-1.57507	0.29066	-1.57507
fDP4 (pH 7.4)	-0.21043	-2.08477	-0.12351	-2.08477
fPP4 (pH 6.8)	-0.09841	-1.65099	-0.05739	-1.65099
fPP4 (pH 7.4)	0.06198	-1.58233	0.11226	-1.58233

Table S3.2.2: List of constant values obtained for different mathematical models during fitting of drug release data.

Fitting	Zero Order	First Order	Higuchi	Hixson-Crowell	Weibull	Korsmeyer-Peppas	
Sample Name	**K0**	**K1**	**K**	**k**	**B**	**k**	**n**
fDP4 (pH 6.8)	1.42E-05	-4.49E+08	0.0027	-6.42E-06	1	0.20198	0.11894
fDP4 (pH 7.4)	9.51E-06	-4.48E+08	0.00185	-3.80E-06	1	0.20661	0.09986
fPP4 (pH 6.8)	5.87E-06	-4.59E+08	0.00115	-2.17E-06	1	0.16174	0.104
fPP4 (pH 7.4)	6.61E-06	-4.59E+08	0.00126	-2.47E-06	1	0.14061	0.12114

Appendix III

Supporting Information

Chapter 3: Results and Discussion (Part III)

Self-assembled Amino acid based copolymer Nanoparticles for Wound Healing and tissue regeneration: structure studied through Molecular Dynamic Simulation

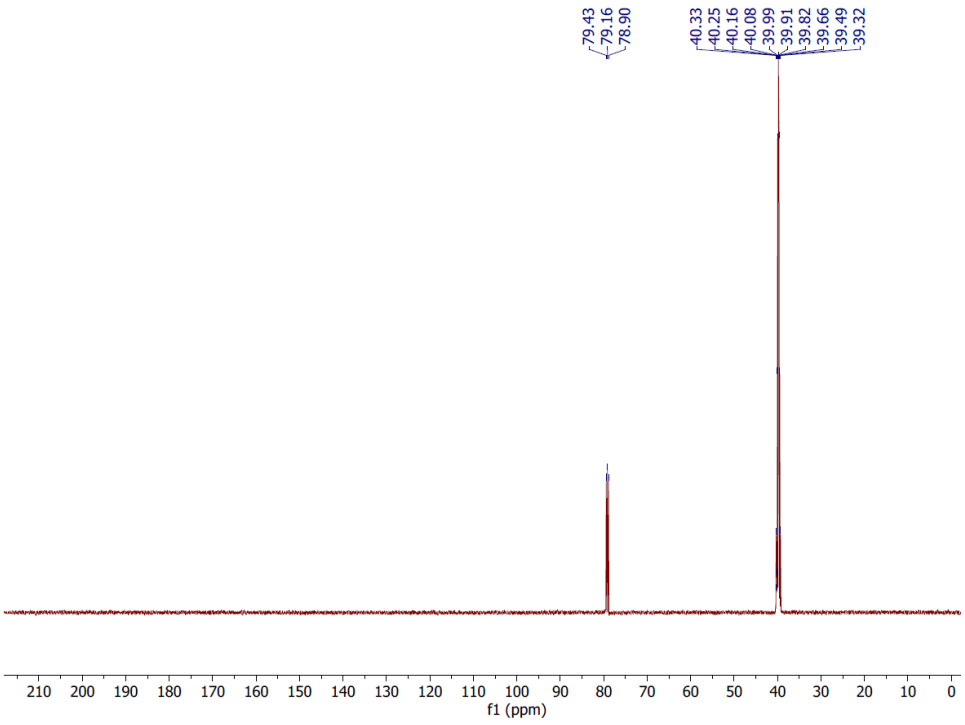

Figure S3.3.1. *^{13}C NMR of p(NAG-co-NAPA)$_{wc}$ NPs.*

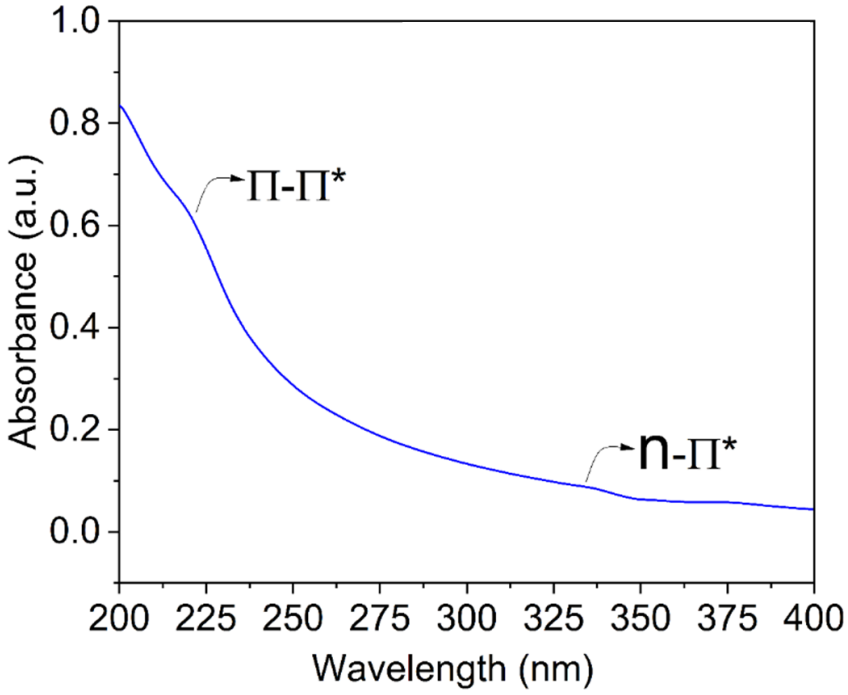

Figure S3.3.2. *UV-Vis spectra of p(NAG-co-NAPA)$_{wc}$ NPs.*

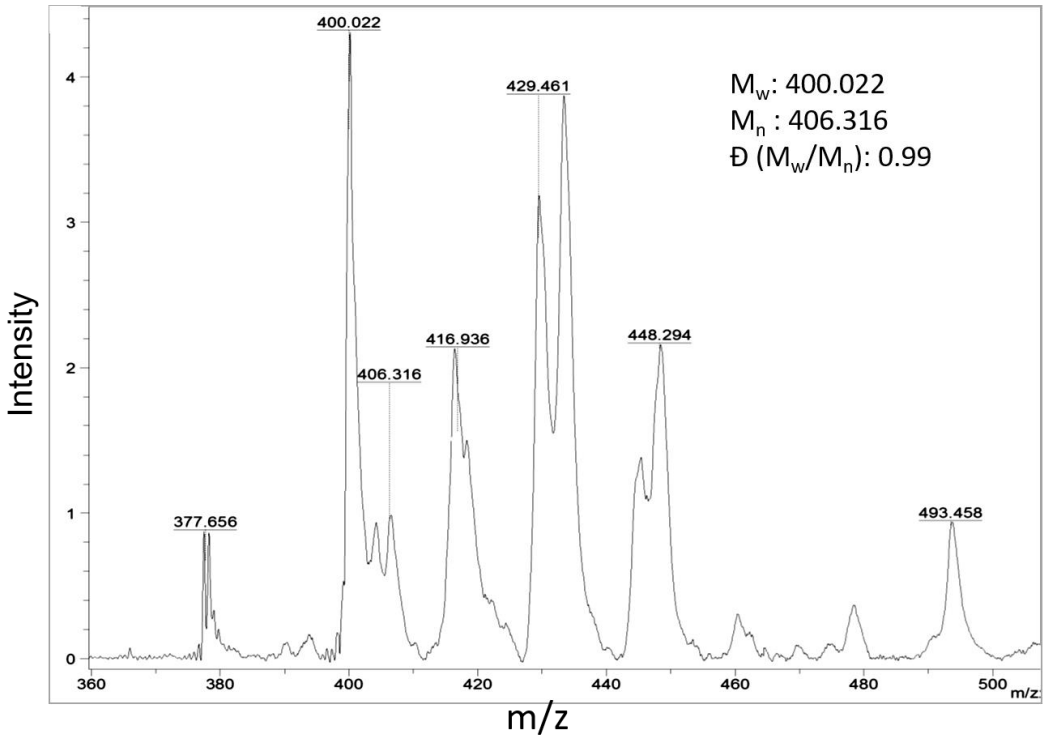

Figure S3.3.3. *MALDI-ToF spectra of p(NAG-co-NAPA)$_{wc}$ NPs.*

(a)

		Size (d.nm):	% Volume:	St Dev (d.nm):
Z-Average (d.nm): 389.0	Peak 1:	578.1	100.0	245.9
PdI: 0.171	Peak 2:	0.000	0.0	0.000
Intercept: 0.970	Peak 3:	0.000	0.0	0.000
Result quality Good				

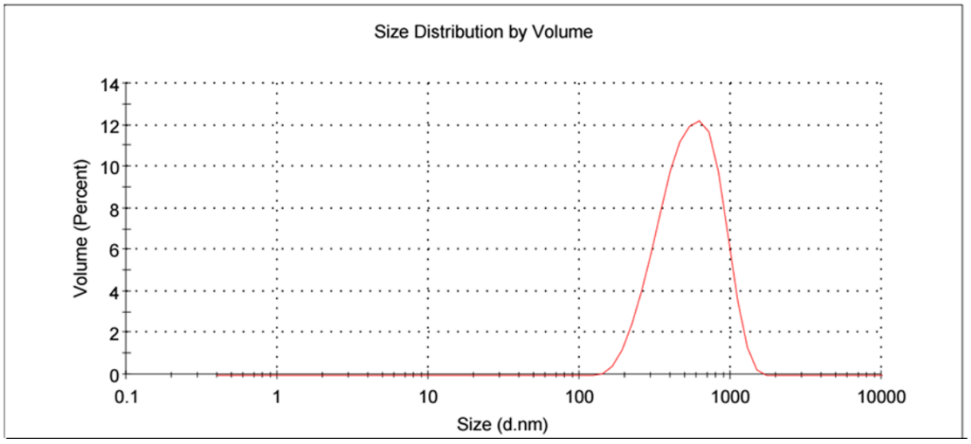

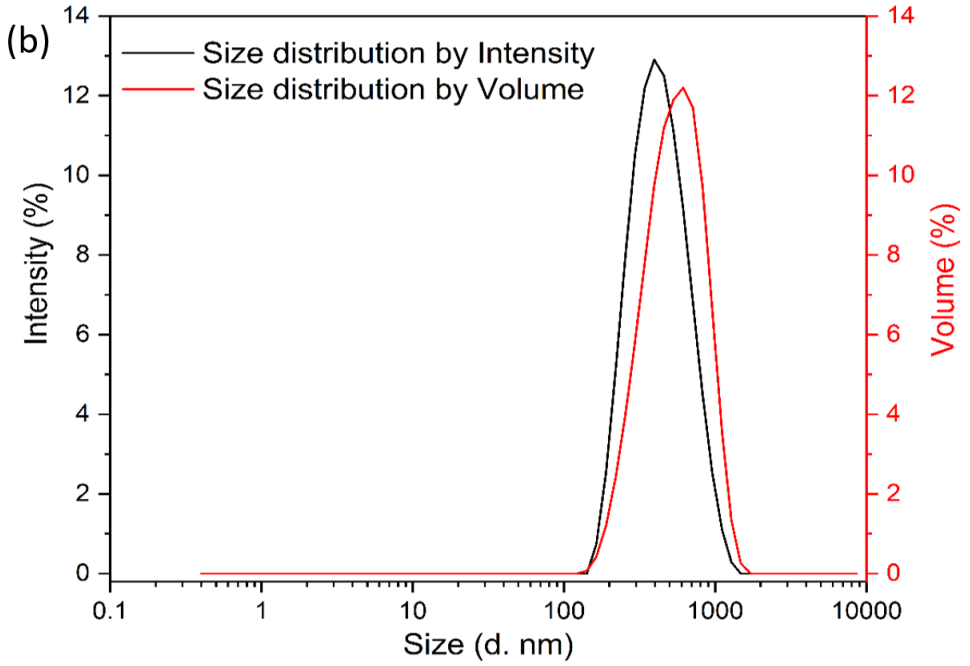

Figure S3.3.4. *(a) Size distribution by volume and (b) Combined plot for Particle size distribution by intensity and Particle size distribution by Volume.*

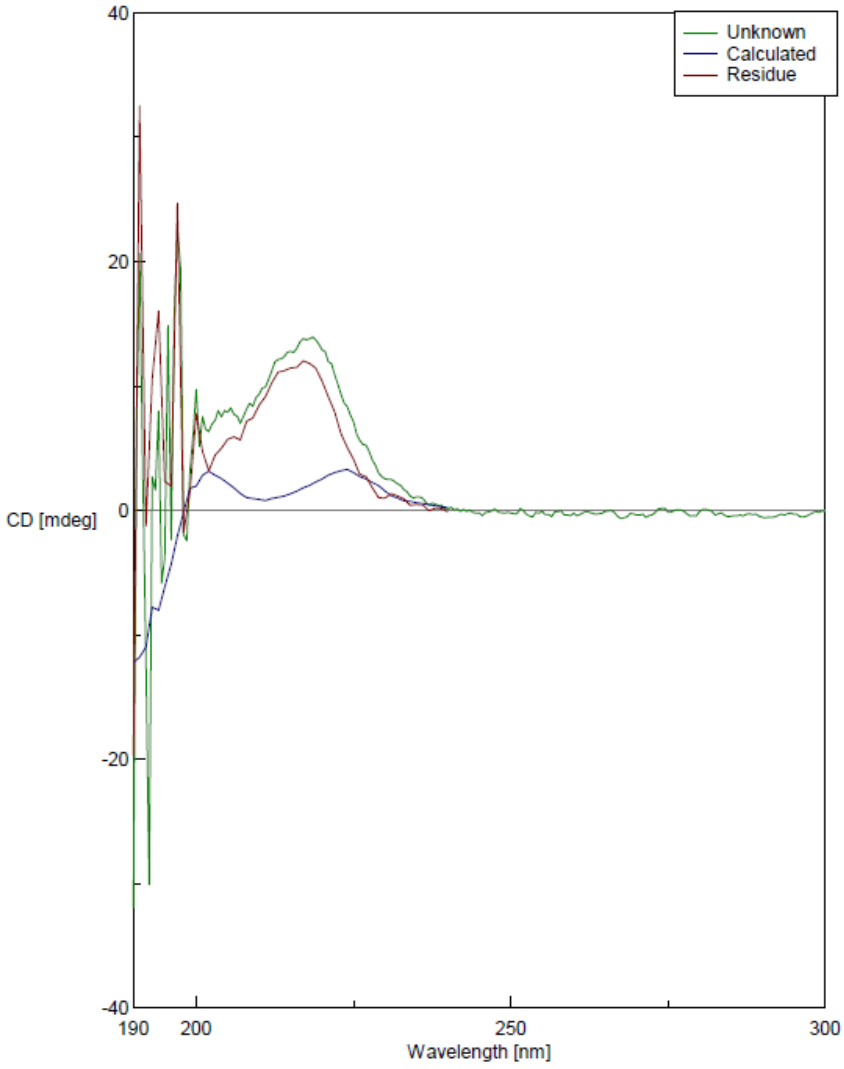

[Analysis Results]

Reference	Yang's Reference	
Finite Mode	Off	
	Fraction	Ratio
Helix	0.0	0.0
Beta	0.0	0.0
Turn	0.0	100.0
Random	0.0	0.0
Total	0.0	100.0
RMS Value	92.298	

Figure S3.3.5. *CD report showing the presence of 100% turns in p(NAG-co-NAPA)$_{wc}$ NP in colloidal state.*

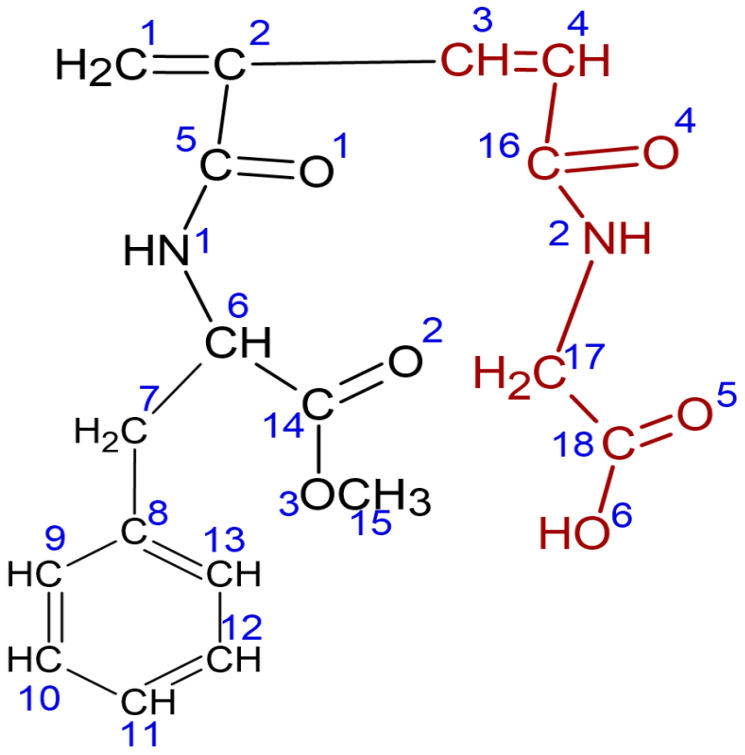

Figure S3.3.6. *Topology of dimer unit (1NAPA-1NAG).*

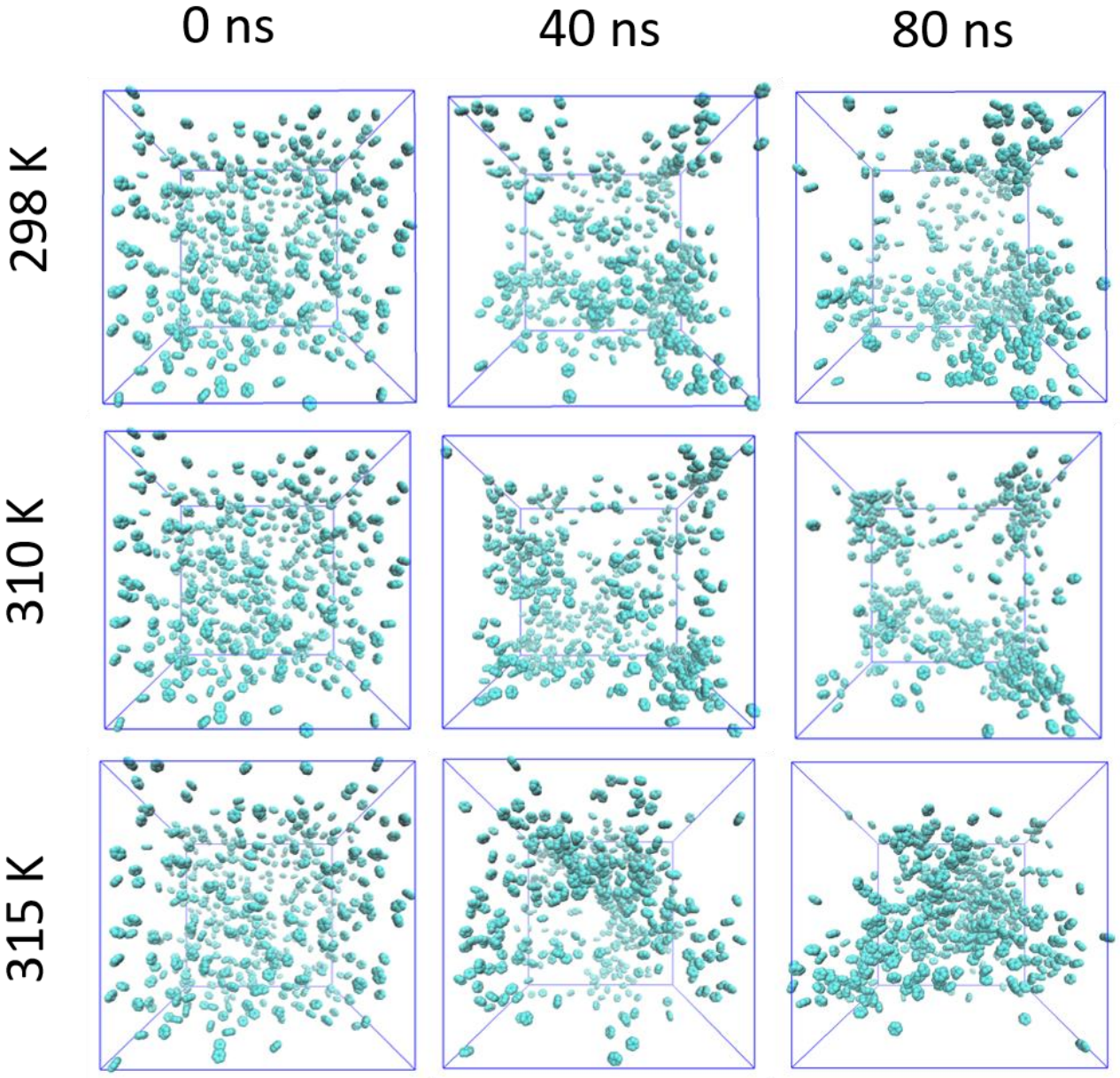

Figure S3.3.7. *Represents the aggregation behavior of hydrophobic phenyl groups present in NAPA units after 0ns, 40ns and 80ns simulation run in three different temperatures (298 K, 310 K and 315 K).*

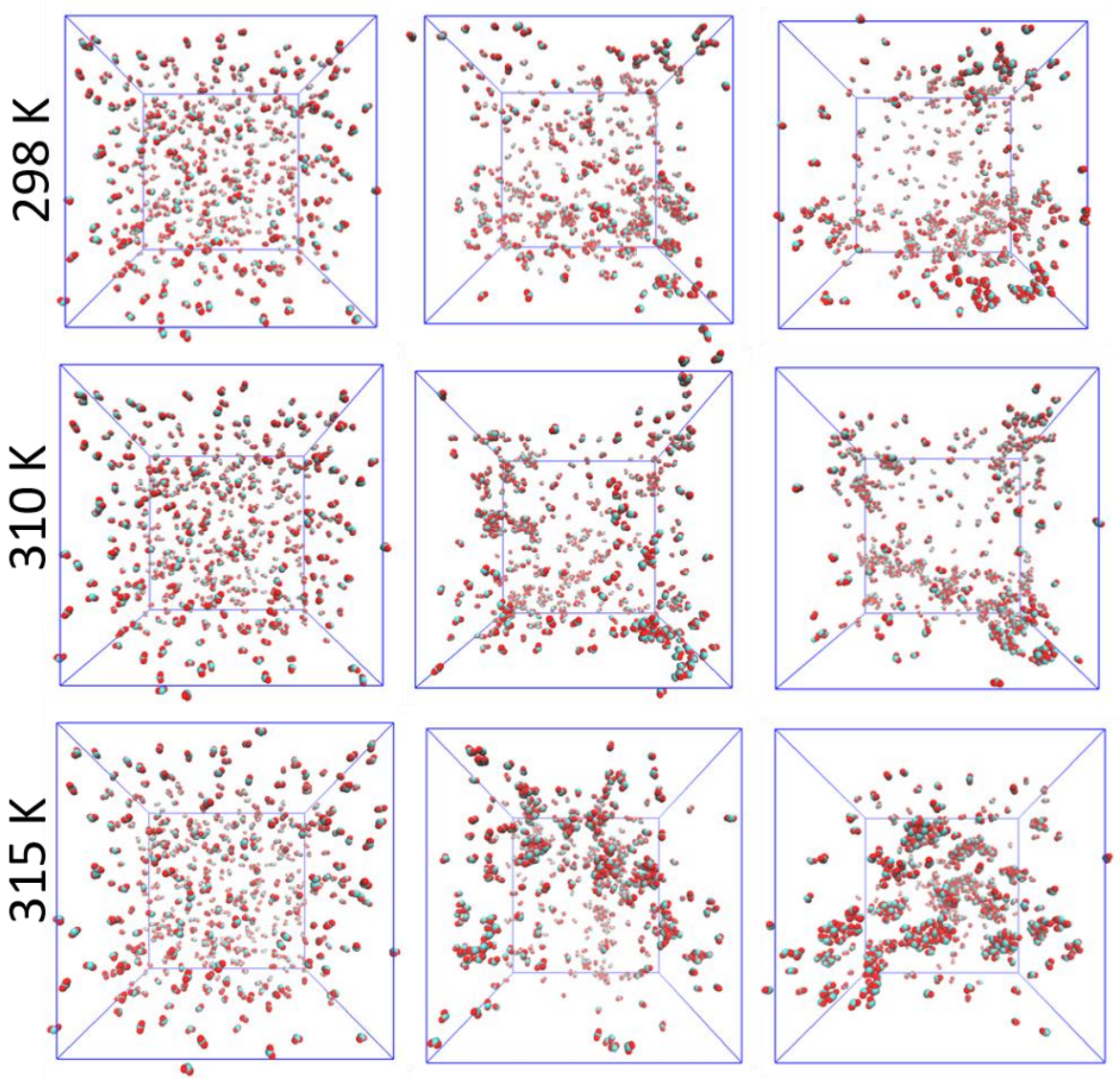

Figure S3.3.8. *Represents the aggregation behavior of hydrophilic carboxyl groups present in NAG units after 0ns, 40ns and 80ns simulation run in three different temperatures (298 K, 310 K and 315 K).*

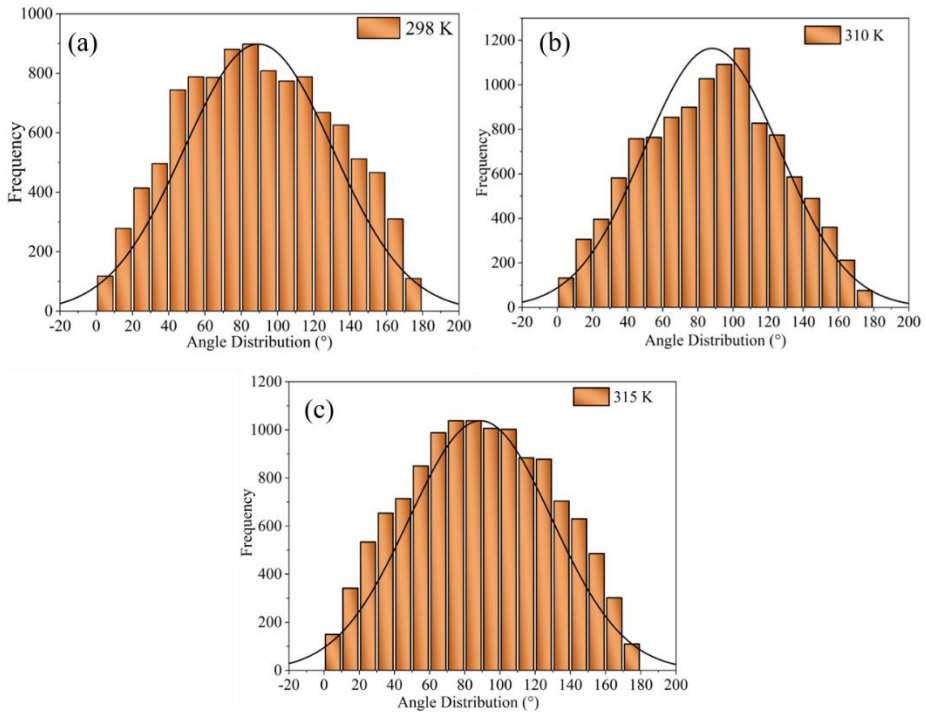

Figure S3.3.9. *Represents angle distribution between* Ph_{14}-Ph_{14} *at (a) 298 K, (b) 310 K, and (c) 315 K.*

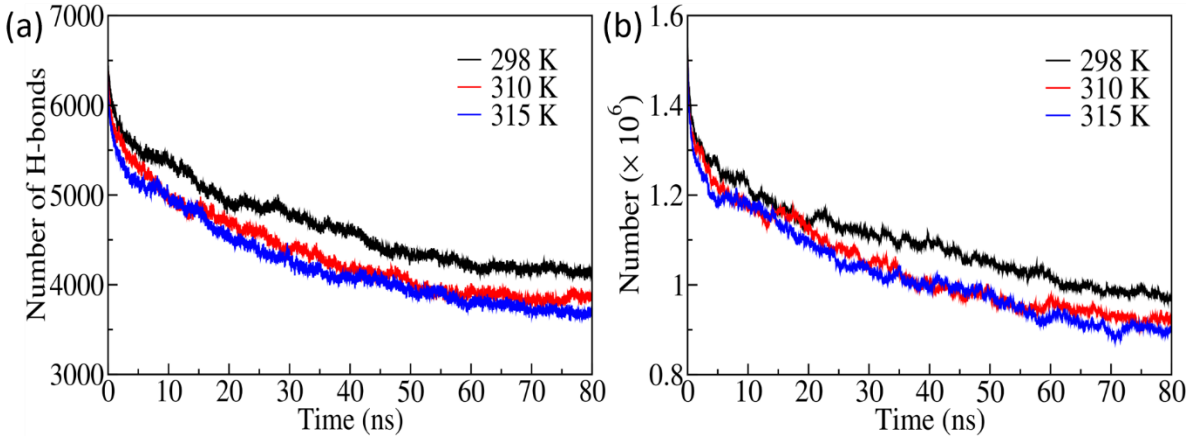

Figure S3.3.10. *Represents (a) Number of Hydrogen bonds, and (b) Number of contacts in between copolymer and water.*

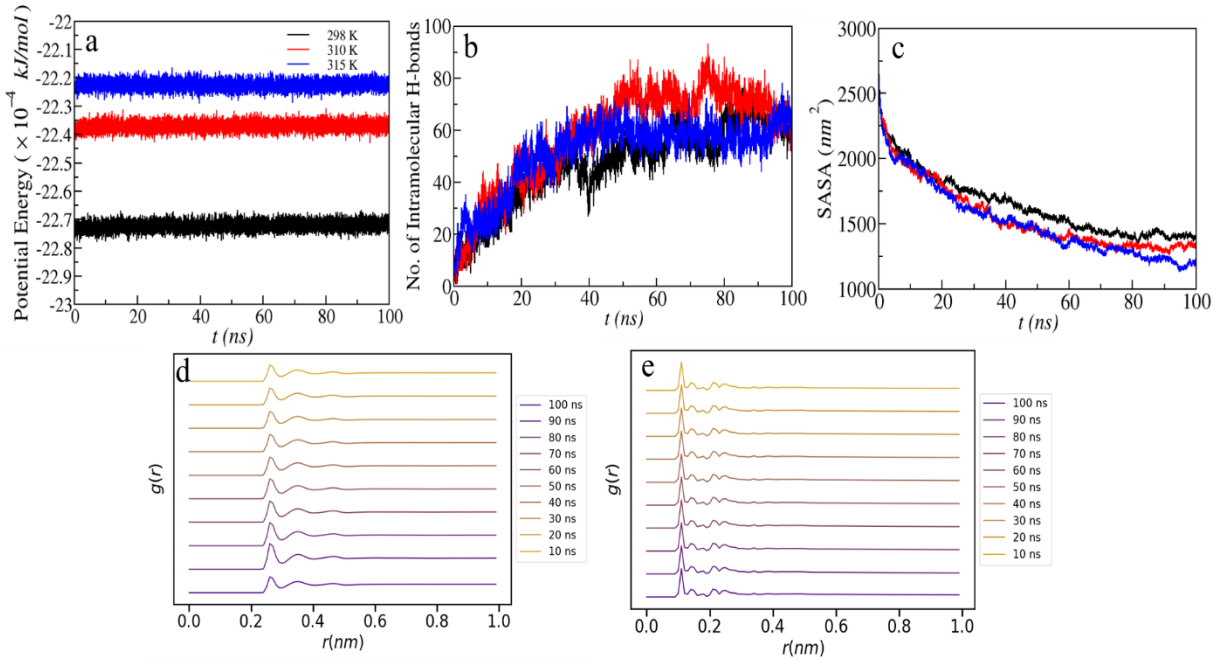

Figure S3.3.11. *Thermodynamic equilibrium properties of the NAG-NAPA dimer system in aqueous media. (a) Potential energy of the system during the production run, (b) Number of intramolecular hydrogen bonds between –COO and –NH atoms, (c) SASA for dimer, at 298, 310 and 315 K in black, red and blue lines respectively, (d) RDF between carboxylic groups of dimer and oxygen atom of water molecules and (e) RDF between dimer units at every 10 ns time intervals.*

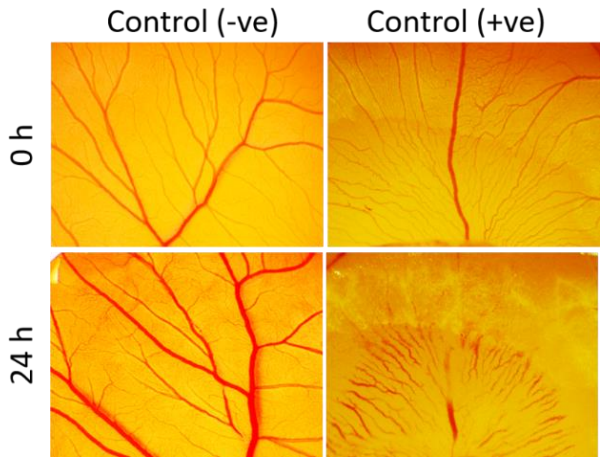

Figure S3.3.12. *Represents the 10x microscopic images of CAM assay acquired to show the irritation effect of formalin in in ovo model after 24 h of treatment.*

Table S3.3.1. Desrciption of system used for MD Simulation.

Temperature	No. of Atoms	Box size(nm)
298 K	164722	11.7639 × 11.7639 × 11.7639
310 K	164722	11.7911 × 11.7911 × 11.7911
315 K	164722	11.8056 × 11.8056 × 11.8056

Table S3.3.2. Represents the ingredients (%) used for oleaginous base preparation.

Sr. No.	Ingredient	Weight (%)
1	Liquid Paraffin	15
2	Paraffin Wax	10
3	Glycerine	5
4	White paraffin wax	45
5	Stearyl alcohol	25
6	Triethanolamine	q.s.

Table S3.3.3. Qualitative assessment of oleaginous base and rBCP NFs.

Sr. No.	Parameters	Required Quality	Oleaginous base	rBCP NFs
1	Appearance	Homogeneous	Homogeneous	Homogeneous
2	Colour	Same as base (white/ up white)	Same as base	Same as base
3	Homogenity	Good	Good	Good
4	Odour	Same as base/ No odour	No odour	No odour
5	Phase Separation	No	No	No

Table S3.3.4. Skin irritation assesssment (Draize score determination).

Value	Erythema Developement	Value	Edema Developement
0	No erythema	0	No edema
1	Extremely minor erythema	1	Extremely minor edema
2	Mild erythema (well defined margins)	2	Mild edema (well defined margins)
3	Moderate severe erythema (Specified colour and erythema region)	3	Moderate severe edema (Specified colour and erythema region)
4	Maximum possible erythema	4	Maximum possible edema

Erythema and Edema are graded in a scale of 0-4. 0 refers to no symptoms whereas 4 refers to sever condition. The average irritation score for each animal was calculated by summing the cutaneous responses recorded at 1, 24, 48, and 72 h after the removal of the ointment. This total value was divided by four to obtain the average score and compared with base and +ve control group.

Appendix IV

Supporting Information

Chapter 3: Results and Discussion (Part IV)

Quantitative Assessment of Angiogenesis via Gray Level Co-occurrence Matrix based Image Processing using poly(*N*-acryloyl-glycine)-*co*-(*N*-acryloyl-*L*-phenylalanine methyl ester) nanoparticles

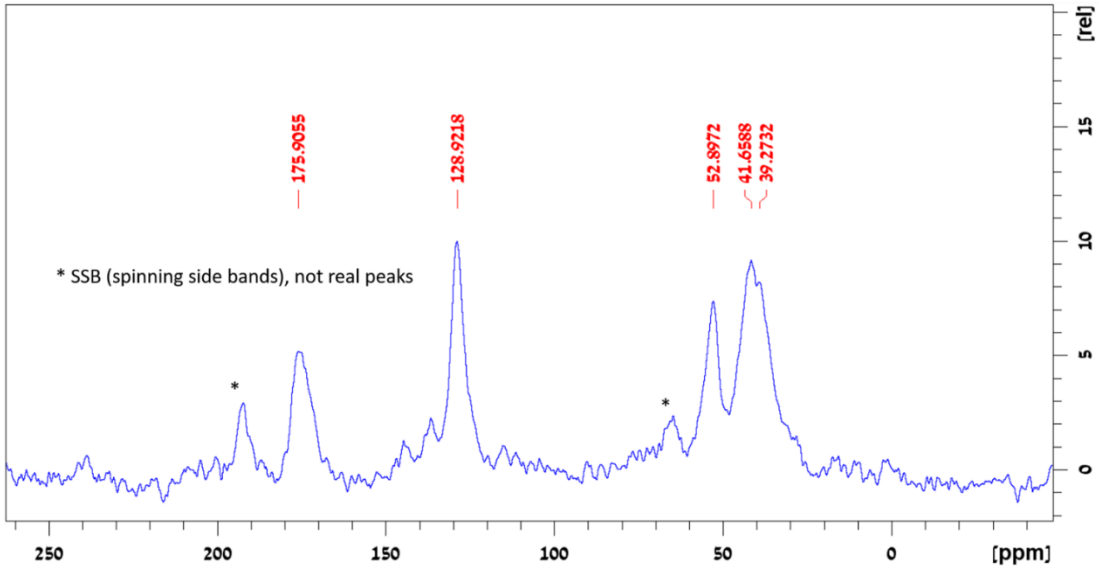

Figure S3.4.1. *^{13}C Solid-state NMR of p(NAG-co-NAPA) NPs.*

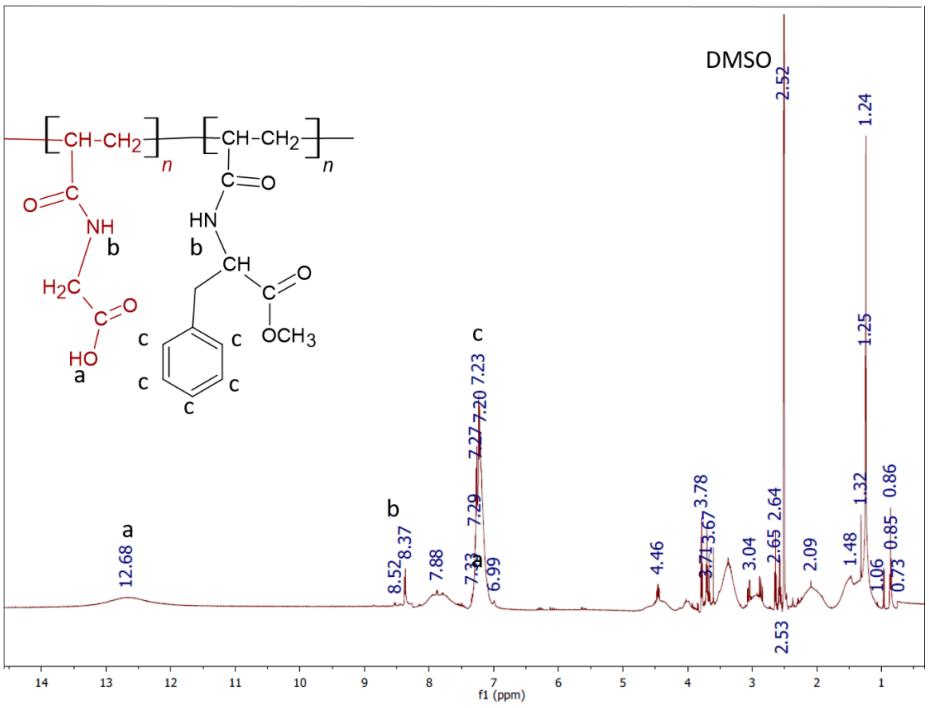

Figure S3.4.2. *^{1}H NMR of p(NAG-co-NAPA)$_{wc}$ NPs.*

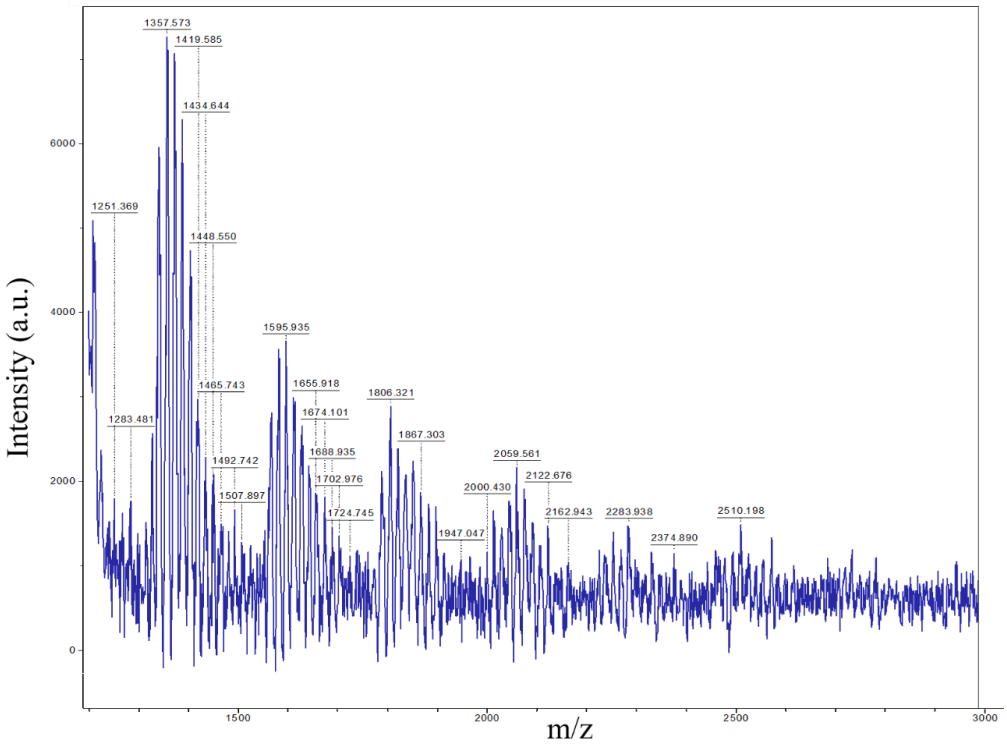

Figure S3.4.3. *Represents the MALDI-ToF spectrum of p(NAG-co-NAPA) NPs.*

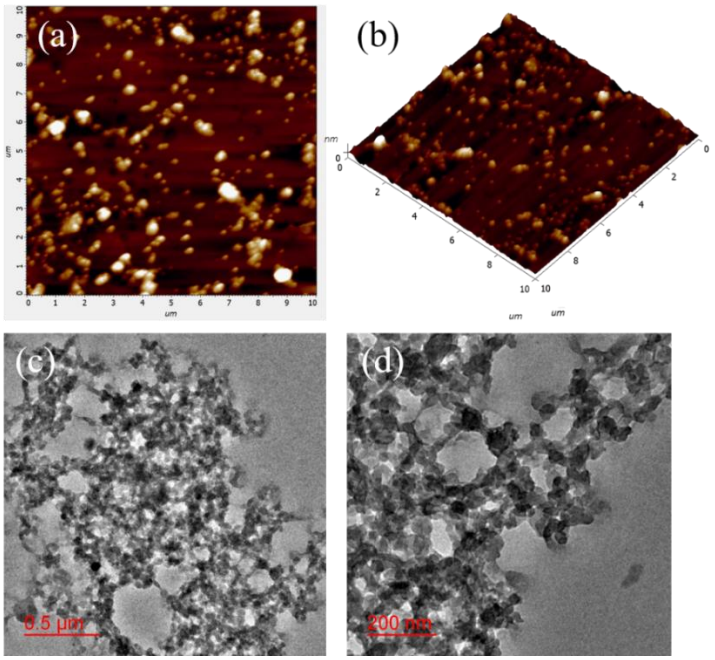

Figure S3.4.4. *Represents the agglomeration behavior of p(NAG-co-NAPA) NPs. (a) 2D and (b) 3D AFM images of p(NAG-co-NAPA) NPs at 10µm scale, (c) and (d) HR-TEM images of p(NAG-co-NAPA) NPs at 500nm at 200nm scale.*

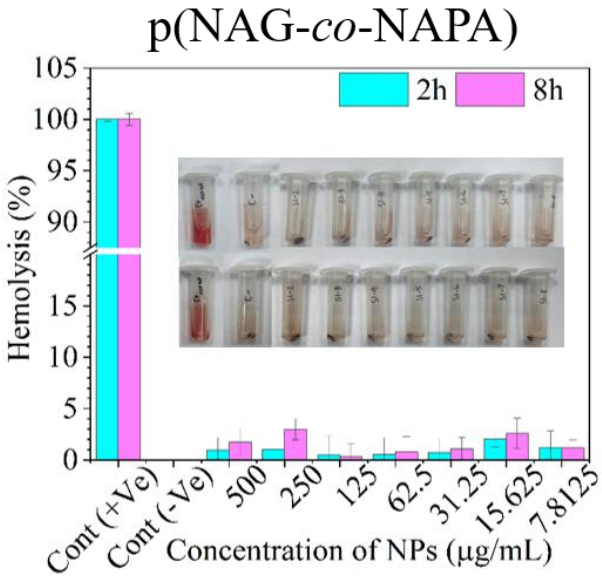

Figure S3.4.5. *Hemolysis (%) of p(NAG-co-NAPA) NPs. At 2h, all concentrations are showing significant difference with control (+ve) with '***' and not significant (ns) with control (-ve). For 8h, all concentrations are showing significant difference with control (+ve) with '***' and only 500µg/mL is showing significant difference with '***'.*

Table S3.4.1. Represents the error% calculated for the Cell Viability study.

Concentration(µg/ml)	L929		RAW 264.7		PC12	
	p(NAPA)	p(NAG)	p(NAPA)	p(NAG)	p(NAPA)	p(NAG)
400	**	*	***	***	NS	NS
200	***	NS	***	**	NS	**
100	**	*	***	NS	**	***
50	NS	NS	**	NS	**	***
25	NS	*	**	NS	**	**
12.5	NS	**	***	NS	NS	***
6.25	NS	NS	***	NS	NS	**
3.125	NS	*	***	NS	NS	**
NS: not significant						

Table S3.4.2. Represents the error% calculated for the Cell Viability study of HUVEC cells.

Concentration(µg/ml)	HUVEC	
	p(NAPA)	p(NAG)
200	***	NS
100	***	NS
50	***	NS
25	***	NS
10	***	NS
5	***	***

Table S3.4.3. Represents the error% calculated for the number of pixels in blood vessels.

Number of pixels in blood vessels					
	Time	**Control**	**1µg**	**10µg**	**100µg**
p(NAPA)	0	3.52675	5.93664	7.51567	4.6627
	2	6.62627	4.21846	8.43219	9.01171
	4	5.94178	7.60607	7.24897	8.83268
	8	5.87941	4.50518	6.12946	2.19371
	24	6.60758	6.49306	7.60039	4.22757
p(NAG)	0	3.52675	2.83613	5.20954	5.07186
	2	6.62627	6.21057	3.21637	8.93945

	4	5.94178	5.34573	7.41008	3.05839
	8	6.87941	3.5753	8.11069	1.41602
	24	6.60758	6.19848	2.19769	2.66008
p(NAG-*co*-NAPA)	0	3.52675	5.99279	5.93664	4.60627
	2	6.62627	8.5375	4.21846	6.69233
	4	5.94178	2.53397	7.60607	0.15441
	8	1.87941	6.56647	4.50518	6.80557
	24	6.60758	5.30111	5.47233	4.22757

Table S3.4.4. Represents the error% calculated for entropy.

Entropy					
	Time	**Control**	**1µg**	**10µg**	**100µg**
p(NAPA)	0	0.2687	3.00098	4.67479	5.62228
	2	0.23154	3.02027	1.54166	8.74816
	4	1.6339	0.80328	0.80328	0.23471
	8	6.11103	1.22809	1.22809	0
	24	2.23361	9.86319	1.98823	0.68837
p(NAG)	0	0.2687	1.77753	2.67502	8.75229
	2	0.23154	4.10935	5.91303	8.09166
	4	1.6339	3.69245	1.86901	7.3602
	8	6.11103	2.32792	8.16248	9.67659
	24	2.23361	2.24231	0.0456	3.0988
p(NAG-*co*-NAPA)	0	0.2687	1.84803	1.10491	1.30726
	2	0.23154	2.74257	1.75127	1.76149
	4	1.6339	2.5652	1.8854	1.05269
	8	1.11103	1.64681	1.20011	0.8244
	24	2.23361	1.87547	0.46794	1.00953

Table S3.4.5. Represents the error% calculated for energy.

Energy					
	Time	**Control**	**1µg**	**10µg**	**100µg**
p(NAPA)	0	0.32712	0.34674	0.48178	1.13853
	2	0.35567	0.10794	0.01964	1.75905
	4	0.48196	0.05104	0.18438	1.31191
	8	1.21795	0.71286	0.6693	0.90657
	24	0.70106	1.3345	0.73627	0.44313
p(NAG)	0	0.32712	0.48806	2.9025	5.90668
	2	0.35567	0.93403	3.276	3.57098
	4	0.48196	0.90663	2.30882	1.60044
	8	1.21795	0.62142	0.62142	2.43274
	24	0.70106	0.87051	0.437	1.15916

p(NAG-*co*-NAPA)	0	0.32712	0.9552	0.58454	0.9515
	2	0.35567	0.94671	0.62175	0.76885
	4	0.48196	0.4541	0.12302	0.23712
	8	0.21795	0.04989	0.55779	0.03195
	24	0.70106	0.67194	0.47245	0.09256

Table S3.4.6. Represents the error% calculated for mean.

Mean					
	Time	**Control**	**1µg**	**10µg**	**100µg**
p(NAPA)	0	0.37834	0.08858	0.08939	1.02228
	2	0.706	0.35098	0.29973	1.70297
	4	0.66174	0.79184	0.4511	1.18151
	8	1.32895	1.18121	0.80708	0.91522
	24	0.92243	0.761	1.00069	0.75472
p(NAG)	0	0.37834	0.51211	3.17444	5.57426
	2	0.706	0.93429	3.49606	3.37725
	4	0.66174	0.91782	2.32817	1.4705
	8	1.32895	0.64209	1.49766	2.45945
	24	0.92243	1.16451	0.31687	1.53266
p(NAG-*co*-NAPA)	0	0.37834	0.34478	0.89598	0.92002
	2	0.706	1.23804	0.59876	0.61953
	4	0.66174	2.44774	1.122	0
	8	1.32895	2.32455	0.74182	0.25276
	24	0.92243	0.70707	0.82282	0.59153

Table S3.4.7. Represents the error% calculated for contrast.

Contrast					
	Time	**Control**	**1µg**	**10µg**	**100µg**
p(NAPA)	0	8.27583	3.79401	19.78922	1.84325
	2	1.93783	2.56206	12.81691	1.72955
	4	4.73547	8.32263	9.05286	9.91213
	8	0.00879	1.72697	2.00665	3.8018
	24	3.97337	2.81178	3.48381	8.5931
p(NAG)	0	8.27583	2.17152	1.5521	3.79834
	2	1.93783	5.51736	2.86597	3.87353
	4	4.73547	5.31102	7.34164	6.1181
	8	0.00879	3.46937	2.85784	1.25676
	24	3.97337	3.12543	5.21121	3.36344
p(NAG-*co*-NAPA)	0	8.27583	8.34478	7.56905	0.62937
	2	1.93783	1.23804	3.30523	4.17939
	4	4.73547	2.44774	5.17778	2.10582
	8	0.00879	2.32455	3.80379	9.79665
	24	3.97337	0.70707	2.34642	9.63705

Table S3.4.8. Represents the error% calculated for dissimilarity.

Dissimilarity					
	Time	**Control**	**1µg**	**10µg**	**100µg**
p(NAPA)	0	1.83837	3.79399	9.78922	1.84325
	2	2.30176	2.56206	2.81689	1.72953
	4	8.00859	8.32263	9.05284	9.912142
	8	0.01535	4.72698	2.00666	3.801778
	24	6.75081	9.81176	2.84194	8.593099
p(NAG)	0	1.83837	2.17152	1.55213	9.92832
	2	9.30176	5.51734	2.86592	3.76089
	4	8.00859	5.311	7.34162	0.38691
	8	0.01535	3.46938	2.85787	2.48895
	24	6.75081	3.12541	3.25788	7.67158
p(NAG-*co*-NAPA)	0	1.83837	8.34478	7.56903	5.25809
	2	1.30176	1.23802	3.30524	7.90467
	4	8.00859	2.44773	5.1778	2.10582
	8	0.01535	2.32456	3.80384	9.79666
	24	6.75081	0.68832	2.34639	9.63705

Table S3.4.9. Represents the error% calculated for variance.

Variance					
	Time	**Control**	**1µg**	**10µg**	**100µg**
p(NAPA)	0	4.45313	0.69318	0.62504	5.52531
	2	8.37644	2.17898	2.02579	1.20718
	4	7.47005	4.99743	2.723	7.47934
	8	4.9442	7.17599	5.02566	5.94283
	24	8.0449	5.53646	4.52934	4.20075
p(NAG)	0	4.45313	0.69318	2.21287	4.68477
	2	8.37644	2.17898	7.00558	8.12007
	4	7.47005	4.99743	8.16824	2.67226
	8	4.9442	7.17599	9.62904	1.23786
	24	8.0449	5.03759	1.88097	3.24895
p(NAG-*co*-NAPA)	0	4.45313	4.00636	5.04335	4.3365
	2	8.37644	9.22113	3.62061	8.20283
	4	7.47005	1.8601	6.48963	7.89355
	8	4.9442	4.38192	3.76462	1.94106
	24	8.0449	1.42344	4.65162	3.63696

Table S3.4.10. Represents the error% calculated for from tube formation assay computed using Angiotool.

p(NAG-*co*-NAPA) NPs	Control	1µg	10µg	100µg
Explant Area	0.628476	0.890086	2.813132	0.539732
Total number of junctions	3.957769	4.845815	3.450317	4.827586
Total vessel length	4.806807483	1.873105287	4.408096894	0.200604492
Mean-E-Lacunarity	3.018299546	1.176093	1.946974	1.209795

Table S3.4.11. Represents the error% calculated for from tube formation assay computed using Image processing tool.

p(NAG-*co*-NAPA) NPs	Control	1µg	10µg	100µg
Number of pixels in blood vessels	2.052102	0.891457	3.939241	1.827812
Entropy	0.886685	0.482057	0.95784	0.466798
Energy	0.362912	0.184573	0.316621	0.363561
Mean	0.530265	0.298528	0.304386	0.692915

Brief on resources used to implement image segmentation and texture feature extraction

The foundational concepts of image processing, including image normalization, smoothing, and blurring, were studied from https://www.geeksforgeeks.org/image-processing-in-python/, which also provided an overview of Python libraries used for image processing. The process of converting RGB images into binary images was implemented using the guidelines from https://www.geeksforgeeks.org/convert-image-to-binary-using-python/ and https://docs.opencv.org/4.x/d7/d4d/tutorial_py_thresholding.html, which detailed the use of OpenCV for thresholding operations. Gaussian adaptive thresholding, a crucial step for precise segmentation, was implemented with the help of https://plantcv.readthedocs.io/en/stable/gaussian_threshold/.

For the analysis of tube formation assay, the code used is https://docs.google.com/document/d/1rFYpgmM1jrImflz7sbFEBu4IjM3J1nnBYX7bkMdY61s/edit?tab=t.0 Additional information on GLCM-based texture features, including contrast, correlation, energy, and homogeneity, was sourced from https://support.echoview.com/WebHelp/Windows_And_Dialog_Boxes/Dialog_Boxes/Variable_Properties_Dialog_Box/Operator_Pages/GLCM_Texture_Features.html and https://scikit-image.org/docs/stable/auto_examples/features_detection/plot_glcm.html.

भारतीय प्रौद्योगिकी संस्थान
काशी हिन्दू विश्वविद्यालय

IIT INDIAN INSTITUTE OF TECHNOLOGY
BANARAS HINDU UNIVERSITY

Department of Pharmaceutical Engineering & Technology

Regd. No. 2123/GO/Re/S/21/CPCSEA

Date: 15 February, 2024

IAEC Approval Number: **IIT(BHU)/IAEC/2024/I/049**

CERTIFICATE

This is to certify that the project proposal entitled ***"Novel Bio-polymeric Nano-formulations for biomedical Applications such as treatment of Diabetic wound and pressure ulcer and Angiogenesis using Rat and mice model"*** submitted by **Mr. Gurmeet Singh** under the supervision of **Dr. Pradip Paik** has been approved/recommended by the IAEC the of Indian Institute of Technology, Banaras Hindu University, Varanasi in its meeting dated **15 February, 2024** and has been sanctioned 50 (M/F **Swiss Albino Mice)** under this proposal for a duration of **12 (Twelve) months.**

Prof. Vikash Kumar Dubey	Dr. Vinod Tiwari	Dr. Shesh Narayan Mishra
Name & Signature	**Name & Signature**	**Name & Signature**
Chairman	**Member Secretary**	**Main Nominee of CPCSEA**

Chairperson
Institutional Animals Ethics Committee
IIT (BHU), Varanasi-221005

Member Secretory
Institutional Animals Ethics Committee
IIT (BHU), Varanasi-221005

Note: The CPCSEA Guideline should be followed strictly while handling the animals.

भारतीय प्रौद्योगिकी संस्थान
काशी हिन्दू विश्वविद्यालय

IIT INDIAN INSTITUTE OF TECHNOLOGY
BANARAS HINDU UNIVERSITY

Department of Pharmaceutical Engineering & Technology

Regd. No. 2123/GO/Re/S/21/CPCSEA

Date: 09 Feb,2023

IAEC Approval Number: **IIT(BHU)/IAEC/2023/048**

CERTIFICATE

This is to certify that the project proposal entitled **"Anti-cancer drugs (Taxol, DOX, Temozolomide, curcumin, Mangiferin etc.) loaded novel bio-polymeric Nano-formulations [(e.g., pNAGA, pNAG NP, pNAFA, pNALA, pNA(F-L)NP, pNA(G-L) NP, PCL, pNIPAM, PVA-Ly and similar samples etc.)] for Biomedical Applications such as anticancer activity against multidrug resistance cancer using Rat and mice model** submitted by **Gurmeet Singh,** under supervision of Dr. Pradip Paik has been approved/recommended by the IAEC of Indian Institute of Technology, Banaras Hindu University, Varanasi in its meeting dated **09 Feb,2023** and has been sanctioned **50 Male/Female Charles Foster mice** under this proposal for a duration of **Twelve (12) months.**

Prof. Vikash Kumar Dubey	Dr. Vinod Tiwari	Dr. Shesh Narayan Mishra
Name & Signature	**Name & Signature**	**Name & Signature**
Chairman	**Member Secretary**	**Main Nominee of CPCSEA**

Note: The CPCSEA Guideline should be followed strictly while handling the animals

Publications and Patents

LIST OF PUBLICATIONS

Journals:

19. Pareek Divya, **Patra Sukanya**, Zeyallua MD, Singh, Gurmeet, Das Taniya, Samata Prakriti, Kudada Aman, Mourya Anjali, Wasnik Kirti, Pradhan Rajalaxmi, Mastai Yithzak, Paik Pradip; Drug free poly(N-acryloyl-L-phenylalanine) nanoparticles for potential treatment of inflammation for selective Organs; ***RSC Journal of Material Chemistry B***, 2025, https://doi.org/10.1039/D5TB00886G

18. Sukanya Patra, Desh Deepak Yadav, Gurmeet Singh, Jyotirmayee, Prakriti Sundar Samanta, Divya Pareek, Aman Srikant Kudada, Anjali Mourya, Debdip Bhandary, Pradip Paik**;** *Self-assembled Amino acid-based copolymer Nanoparticles for Wound Healing and tissue regeneration: structure studied through Molecular Dynamic Simulation***, *RSC Nanoscale*, 2025,** https://doi.org/10.1039/D5NR00281H

17. Sukanya Patra, Jyotirmoyee, Krishan Kumar, Divya Pareek, Prem Shankar Gupta, Anjali Mourya, Taniya Das, Kirti Wasnik, Malkey Verma, Ruchi Chawla, Tarun Batra,Organ Targeting Drug Delivery Systems (OTDDS) of poly[(N-acryloyl glycine)-co-(N-acryloyl-L-phenylalanine methyl ester)] Copolymer Library and Effective treatment of Triple Negative Breast Cancer; ***RSC Journal of Materials Chemistry B***, 2025;13(9):3876-3894

16. Pareek D, Zeyaullah M, **Patra S**, Alagu O, Singh G, Wasnik K, Gupta PS, Paik P. Mesoporous polymeric nanoparticles for effective treatment of inflammatory diseases: an in vivo study. ***Journal of Materials Chemistry B***. 2025;13(9):3094-113.

15. Wasnik K, Singh G, Yadav DD, **Patra S**, Gupta PS, Oviya A, Kumar S, Pareek D, Paik P. Poly [(N-acryloyl glycine)-co-(acrylamide)]-induced cell growth inhibition in heparanase-driven malignancies. ***Nanoscale***. 2025;17(14):8544-62.

14. Somedutta Maity, Santhosh Kumar, Gurmeet Singh, **Sukanya Patra**, Divya Pareek, Pradip Paik; Selective sensing of heavy metal ions using carbon dots synthesized from Azadirachta indica seeds", ***RSC Sensors & Diagnostics***

13. Amgoth C, Pareek D, **Patra S** and et al.;Block-Co-Polymer based Discoid type porous Capsules as Potential Payload for Multiple Anticancer Drugs and proteins, ***Journal of Applied Polymer Science***, *26th May 2024 (Submitted)*

12. Patra S, Pareek D, Gupta PS, Wasnik K, Singh G, Yadav DD, Mastai Y, Paik P. Progress in Treatment and Diagnostics of Infectious Disease with Polymers. ***ACS Infectious Diseases***. 2024 Jan 18;10(2):287-316.

11. Wasnik K, Gupta PS, Singh G, Maity S, **Patra S**, Pareek D, Kumar S, Rai V, Prakash R, Acharya A, Maiti P. Neurogenic and angiogenic poly (N-acryloylglycine)-co-(acrylamide)-co-(N-acryloyl-glutamate) hydrogel: preconditioning effect under oxidative stress and use in neuroregeneration. ***Journal of Materials Chemistry B***. 2024;12(25):6221-41.

10. Gupta PS, Wasnik K, **Patra S**, Pareek D, Singh G, Yadav DD, Maity S, Paik P. Nitric oxide releasing novel amino acid-derived polymeric nanotherapeutic with anti-inflammatory properties for rapid wound tissue regeneration. ***Nanoscale***. 2024;16(4):1770-91.
9. Wasnik K, Gupta PS, Mukherjee S, Oviya A, Prakash R, Pareek D, **Patra S**, Maity S, Rai V, Singh M, Singh G. Poly (N-acryloylglycine-acrylamide) Hydrogel Mimics the Cellular Microenvironment and Promotes Neurite Growth with Protection from Oxidative Stress. ***ACS Applied Bio Materials***. 2023 Nov 22;6(12):5644-61.
8. Gupta PS, Wasnik K, Singh G, **Patra S**, Pareek D, Yadav DD, Tomar MS, Maiti S, Singh M, Paik P. In vivo potential of polymeric N-acryloyl-glycine nanoparticles with anti-inflammatory activities for wound healing. Materials Advances. 2023;4(20):4718-31. ***RSC Mater. Adv.***, 2023,4, 4718-4731.
7. Amgoth C, **Patra S**, Wasnik K, Maity P, Paik P. Controlled synthesis of thermosensitive tunable porous film of (pNIPAM)-b-(PCL) copolymer for sustain drug delivery. ***Journal of Applied Polymer Science***. 2023 May 20;140(20):e53854.
6. Maity S, Tomar MS, Wasnik K, **Patra S**, Modak MD, Gupta PS, Pareek D, Singh M, Paik P. Azadirachta indica Seed Derived Carbon Nanocapsules: Cell Imaging, Depolarization of Mitochondrial Membrane Potential, and Dose-Dependent Control Death of Breast Cancer. ***ACS Biomaterials Science & Engineering***. 2022 Jul 27;8(8):3608-22.
5. Panigrahi G, Medhi H, Wasnik K, **Patra S**, Gupta P, Pareek D, Maity S, Mandey M, Paik P. Hollow mesoporous SiO2–ZnO nanocapsules and effective in vitro delivery of anticancer drugs against different cancers with low doses of drugs. ***Materials Chemistry and Physics***. 2022 Aug 1;287:126287.

4. Pandey M, Wasnik K, Gupta S, Singh M, **Patra S**, Gupta P, Pareek D, Maity S, Tilak R, Paik P. Targeted specific inhibition of bacterial and Candida species by mesoporous Ag/Sn–SnO 2 composite nanoparticles: In silico and in vitro investigation. ***RSC advances***. 2022;12(2):1105-20.

3. Pandey M, Singh M, Wasnik K, Gupta S, **Patra S**, Gupta PS, Pareek D, Chaitanya NS, Maity S, Reddy AB, Tilak R. Targeted and enhanced antimicrobial inhibition of mesoporous ZnO–Ag2O/Ag, ZnO–CuO, and ZnO–SnO2 composite nanoparticles. ***ACS omega***. 2021 Nov 16;6(47):31615-31.

2. **Patra S**, Singh M, Wasnik K, Pareek D, Gupta PS, Mukherjee S, Paik P. Polymeric nanoparticle based diagnosis and nanomedicine for treatment and development of vaccines for cerebral malaria: a review on recent advancement. ***ACS Applied Bio Materials***. 2021 Sep 15;4(10):7342-65.
1. Amgoth C, Dharmapuri G, **Patra S**, Wasnik K, Gupta P, Kalle AM, Paik P. 'Plate-like-coral'polymer particles with dendritic structure and porous channels: Effective delivery of anti-cancer drugs. ***Journal of Applied Polymer Science***. 2021 May 15;138(19):50386.

Manuscript Communicated/ to be communicated

1. **Sukanya Patra**, Aniket Lokhande, Gurmeet Singh, Divya Pareek, Anjali Mourya; Jac Fredo Ronickom, Pradip Paik, Synthesis of poly(N-acryloyl-phenylalanine methyl ester)-co-(N-acryloyl-glycine) copolymer and angiogenesis study through Gray Level Co-occurrence Matrix for therapeutic uses; ***RSC Materials Advances***,(Submitted)
4. **Sukanya Patra**, Pradip Paik; Co-delivery of Dihydroartemisinin and Piperine by Folate decorated poly[(*N*-acryloyl glycine)$_1$-co-(*N*-acryloyl-*L*-phenylalanine methyl ester)$_4$] copolymer for Triple Negative Breast Cancer Treatment (to be communicated)

Patents Filed/ Published/ Granted:

12. Pradip Paik, Divya Pareek, **Sukanya Patra** "*A process of Preparation of poly-Tryptophan thereof*" (application pending, 2024)

11. Pradip Paik, **Sukanya Patra**, A. R. Jac Fredo, Aniket Dayanand Lokhande '*Quantitative Assessment of Angiogenesis via Gray Level Co-Occurrence Matrix Based Image Processing*' Application No. 202511050871, Dated 27 May, 2025

10. Pradip Paik, **Sukanya Patra** '*A Polymeric Nanoformulation and a Method of Synthesis Thereof*' *Patent Application No.: 202511082570,* August 30, 2025

9. Pradip Paik, **Sukanya Patra**, Divya Pareek, Desh Deepk Yadav '*A plurality of self-assembled copolymer nanoparticles and a method of synthesis thereof*'. Patent Application no.: 202511043769, Dated: 6th May 2025

8. Pradip Paik and **Sukanya Patra** '*A polymeric nanocapsule and a method of synthesis thereof'. Patent Application No.:* ***202511034476****,* April 08, 2025'

7. Pradip Paik, Prem shankar Gupta, Kirti Wasnik, **Sukanya Patra**, Divya Pareek, '*A Polymeric Nanoparticle Formulation and A Method of Preparation Thereof*', Patent Application No.: 202311041625, June 19, 2023 **(Granted)**
6. Pradip Paik, Kirti Wasnik, Prem Shankar Gupta, **Sukanya Patra**, Divya Pareek, Gurmeet Singh, '*A polymeric nano-hydrogel composition and a method of preparation thereof*'. Patent Application No.: 202311038604, Date of filing: June 5th, 2023
5. Pradip Paik, Monica Pandey, Monika Singh, **Sukanya Patra**. '*Mesoporous nano-inorganic antibiotic compositions and method of preparation thereof*', 202211015312, Dated: March 21, 2022 **(Granted)**
4. Pradip Paik, Monica Pandey, Monika Singh, **Sukanya Patra**, '*Quaternary antibiotic composition and method of preparation thereof*', 202211015313, Dated: March 21, 2022 **(Granted)**
3. Pradip Paik, Monika Singh, Shilpa Jaiswal, **Sukanya Patra**, Nira Mishra, 'A biomaterial-based composition and a method of preparation thereof', Application No.: 202311065055, September 27, 2023

2. Pradip Paik, Debasrita Bharatis, **Sukanya Patra**, '*Biocompatible nano-triblock-co-polymers and a process for their preparation'*, Application No.: 202011029248, (9th, July 2020) **(Granted)**

1. Pradip Paik, Monica Pandey, Kirti Wasnik, Prem Shankar Gupta, Monika Singh, **Sukanya Patra**, '*A mesoporous anti-microbial nanocomposite and a method of preparation thereof*', Application No.: 202011031802, dated: July 24, 2020. **(Granted)**

Book Chapters:

5. **Sukanya Patra**#, Monika Singh#, Divya Pareek, Kirti Wasnik, Prem Shankar Gupta, Pradip Paik*, 2022, Advances in the Development of Biodegradable Polymeric Materials for Biomedical Applications. In: Hashmi, M.S.J. (ed.) Encyclopedia of Materials: Plastics and Polymers, vol. 4, pp. 532–566. Oxford: Elsevier.
4. Prem Shankar Gupta #, Kirti Wasnik #, **Sukanya Patra**, Divya Pareek, Monika Singh, Somedutta Maity, Monica Pandey, Pradip Paik*, 2022, A Review on Biodegradable Polymeric Materials for Bone Tissue Engineering (BTE) Applications. In: Hashmi, M.S.J. (ed.) Encyclopedia of Materials: Plastics and Polymers, vol. 4, pp. 498–531. Oxford: Elsevier.
3. Monika Singh, **Sukanya Patra**, Rajesh Kumar Singh. Common techniques and methods for screening of natural products for developing of anticancer drugs. In Evolutionary diversity as a source for anticancer molecules 2021 Jan 1 (pp. 323-353). Academic Press.
2. Aman Srikant Kukada, Gurmeet Singh, Divya Pareek, Desh Deepak Yadav, **Sukanya Patra**, Anjali Prasad Mourya, Taniya Das, Kirti Wasnik and Pradip Paik, Elsevier Reference Module in Materials Science and Materials Engineering.
1. **Sukanya Patra**, Jyotirmayee, Pradip Paik and Malkhey Verma; Unlocking the Secrets of the King of Spices: Exploring Its Chemistry, Health Benefits and Medicinal Wonders, CRC Press/Taylor & Francis group (Submitted).

Conferences, Workshops and Webinars:

19. Stimuli responsive polymer for antibacterial and therapeutic applications, Debasrita Bharatiya, **Sukanya Patra**, Pradip Paik, Emerging Trends and Techniques in Medicinal chemistry-2020 (ETTMC-2020), March, 2020, Central University of Gaya,Bihar

18. Delivery of Nitric Oxide Through Polymer Nanoparticles for Chronic Wound Healing, Prem Shankar Gupta, Kirti Wasnik, Divya Pareek, **Sukanya Patra**, Dr. Monika and Pradip Paik, ICNOC 2022, Jamia-Miliya Ishlamia, New Delhi
17. Nitric oxide-releasing polymeric nanotherapeutics for wound healing, Prem Shankar Gupta*, Kirti Wasnik, Divya Pareek, **Sukanya Patra**, Dr. Monika and Pradip Paik, SPSI-MACRO-2022, CSIR - NCL, Pune
16. Gas Therapy for Chronic Wound Healing, Perm Shankar Gupta*, Kirti Wasnik, **Sukanya Patra**, Divya Pareek, Dr. Monika and Dr. Pradip Paik, AMFP-2022, Dr. B. R. Ambedkar NIT Jalandhar, SLIET Longowal, Université de Bejaia, DIAT Pune
15. Novel Nanopolymer for poor prognosis cancer treatment without Conventional Drugs in heparanase driven malignancies, Kirti Wasnik, Prem Sankar Gupta, Alagu Oviya, Saurabh Kumar Yadav, Sandeep Singh, **Sukanya Patra**, Divya Pareek, Pradip Paik, ICDD-2022, BITS Pilani, Goa
14. Anti-tumorigenic Characteristics of Poly (N-acryloyl-glycine-acrylamide) Co-polymeric Hydrogel, Kirti Wasnik, Prem Sankar Gupta, Divya Pareek, **Sukanya Patra**, Pradip Paik, SPSI-MACRO-2022, CSIR - NCL, Pune

13. Controlled synthesis of thermosensitive tunable porous polymeric film of (pNIPAM)-*b*-(PCL) for sustain drug delivery, **Sukanya Patra**, Chander Amgoth, Kirti Wasnik, Divya Pareek, Pradip Paik,BioHeal-2023, Parmarth Niketan, Rishikesh,Uttarakhand (**Student Intelligent Award**)

12. Amino acid-based polymer nanocapsules showing sustained drug release and immunostimulatory effect on macrophages, Divya Pareek, **Sukanya Patra**, Prem Shankar Gupta, Kirti Wasnik, Gurmeet Singh, Desh Deepak Yadav, Pradip Paik, BioHeal-2023, Parmarth Niketan, Rishikesh,Uttarakhand

11. Thermosensitive porous polymeric film for control drug delivery, **Sukanya Patra**, Chander Amgoth, Prem Shankar Gupta , Kirti Wasnik, Divya Pareek, Pradip Paik, ICNP-2023,Kerala
10. Amino acid based Polymer Nanocapsule stimulate naïve macrophages and protect them from oxidative damage during controlled drug release, Divya Pareek, Kirti Wasnik, Prem Shankar Gupta, **Sukanya Patra**, Desh Deepak Yadav, Yitzhak Mastai, Pradip Paik, Michael Sela Memorial Syposium, June 2023, Weizmann Institute of Science, Rehovat, Israel
9. Enhancing Immune Efficiency Through Amino Acid-Based Polymeric Nanoparticles Divya Pareek**, Sukanya Patra**, Kirti Wasnik, Algu Oviya, Desh Deepak Yadav, Gurmeet Singh, Amam Srikant Kudada, Pradip Paik Presented at International Conference on POLYMERS FOR ADVANCED TECHNOLOGY, APA-2024, Jaipur, 16-18 October 2024
8. Organ Targeting Drug Delivery Systems (OTDDS) of poly[(*N*-acryloylglycine)-*co*-(*N*-acryloyl-L-phenylalanine methyl ester)] Copolymer Library and Effective treatment of Triple Negative Breast Cancer, **Sukanya Patra**, Divya Pareek, Pradip Paik, National Biomedical Research Competition, NBRCOM 2024, AIIMS Delhi, 1-3 December 2024

7. Multifunctional Self-assembled Amino acid based Block Copolymer for Wound healing: validate through MD simulation and *in vivo* rat model, **Sukanya Patra**, Desh Deepak Yadav, Debdip Bhandary, Pradip Paik, PAN-IIT Meet and Conference on Engineering in Medicine, IIT Kanpur, 6-8 December 2024 (Merck Life Science Best Poster Award in Digital Medicine)

6. Hollow-Mesoporous Polymeric nanomedicine for efficient treatment of Inflammatory Diseases: an in vivo study Divya Pareek, **Sukanya Patra**, Gurmeet Singh, Desh Deepak Yadav, Oviya Algu, Pradip Paik Presented at PAN-IIT Meet, IIT Kanpur, 6-8 December 2024

5. BSL-3 Laboratory training and handling practices for mycobacterium tuberculosis (19^{th} -25^{th} July 2021) organized by the Department of Biochemistry, University of Delhi South campus.

4. The "Confocal Microscopy" workshop was organized by SATHI, BHU, Varanasi (26^{th} -27^{th} April 2022).

3. Webinar on "Animal model-based techniques" organized by Jackson Laboratory.

2. 4th Online International Flow Cytometry Course, 22nd-24th September 2023(Basic Course).

1. Online computational chemistry training/workshop, CCG, 24^{th} to 29^{th} Jan 2022.

Nanoscale

PAPER

View Article Online
View Journal

Cite this: DOI: 10.1039/d5nr00281h

Self-assembled amino acid-based copolymer nanoparticles for wound healing and tissue regeneration: structure studied through molecular dynamic simulation

Sukanya Patra,[a] Desh Deepak Yadav,[a] Gurmeet Singh,[a] Jyotirmayee,[b] Prakriti Sundar Samanta,[a] Divya Pareek,[a] Aman Srikant Kudada,[a] Anjali Ramsabad Mourya,[a] Debdip Bhandary *[c] and Pradip Paik *[a]

Amino acid-based block copolymer nanoparticles with cross-linkers have garnered growing interest in recent years. However, its intricate synthesis and purification difficulties, along with stability concerns linked to intermicellar crosslinking, restrict their potential use in healthcare and therapeutic applications. Thus, the present work aimed to design amphiphilic block copolymer nanoparticles of *N*-acryloyl glycine and *N*-acryloyl-(L-phenylalanine methyl ester), *i.e.*, p(NAG-*co*-NAPA)$_{wc}$, without the use of a crosslinker *via* miniemulsion free radical polymerization. The self-assembled π–π stacking structural arrangement of the copolymer at different temperatures has been confirmed through molecular dynamics (MD) simulations, which corroborated the structural stability of the copolymer nanoparticles at physiological temperature (37 °C). The cell migration results of the p(NAG-*co*-NAPA)$_{wc}$ nanoparticles are complementary to those of the CEMA assay, revealing their tissue regeneration properties. Furthermore, the *in vivo* wound healing study demonstrated that within 13 days post-treatment, ~97% of the wound can be healed, whereas for the control, it was found to be only ~80%. Additionally, the RT-PCR results revealed that the p(NAG-*co*-NAPA)$_{wc}$ nanoparticles possess anti-inflammatory and tissue regeneration properties by downregulating TNF-α and IL-1β and upregulating PECAM-1 and VEGF-A, respectively. In conclusion, these p(NAG-*co*-NAPA)$_{wc}$ nanoparticles are paramount with an extensive clinical potential for the regeneration of acute wounds and can be used for other therapeutic applications.

Received 20th January 2025,
Accepted 29th July 2025

DOI: 10.1039/d5nr00281h

rsc.li/nanoscale

Introduction

Amino acid-based random block copolymers have gained much attention in biomedical applications due to their unique structures and molecular properties. Block copolymers can be self-assembled into various stable nano-objects based on the applied conditions.[1,2] They can be conjugated with biomolecules, such as drugs or genetic materials, or encapsulated through absorption/adsorption or chemical reactions on their surface or in the void space.[3,4] Their biocompatibility and high bioavailability have received considerable attention over other properties.[5] The presence of hydrophilic/hydrophobic functional groups in the polymer chains facilitates the smart attachment of other multiple blocks, which subsequently helps in developing surface multi-functionality, high crosslinking, interlocking or branching structure, excellent solubility and a symmetric effect. Furthermore, the degradation of their secondary bonds causes pore formation, which may exert influences by varying the temperature, humidity, solvent and pH.[6]

Self-assembly, hydrothermal synthesis, phase separation, reversed atom transfer radical polymerization, and mini/macro emulsion radical polymerizations are often used to synthesize polymer nanoparticles. Crosslinkers play a major role in minimizing premature disintegration and providing prolonged circulation time with the controlled release of biomolecules.[7,8] Polymeric nanoparticles with chemically bonded crosslinkers are more stable in high dilutions due to their complex interconnected network. However, they show poor response to any external stimuli and self-healing. Excessive use of crosslinkers makes the polymeric particle rigid and can cause severe toxicity to organs.[9] Furthermore, crosslinkers are highly chemically active and tend to bind with the endothelial cells, body

[a]*School of Biomedical Engineering, Indian Institute of Technology (BHU) Varanasi, Uttar Pradesh, 221 005, India. E-mail: paik.bme@iitbhu.ac.in*
[b]*School of Biotechnology, Institute of Science, Banaras Hindu University, Varanasi, 221 005 Uttar Pradesh, India*
[c]*Department of Chemical Engineering and Technology, Indian Institute of Technology (BHU) Varanasi, Uttar Pradesh, 221 005, India. E-mail: debdip.che@iitbhu.ac.in*

Journal of Materials Chemistry B

ROYAL SOCIETY OF CHEMISTRY

PAPER

View Article Online
View Journal | View Issue

Cite this: J. Mater. Chem. B, 2025, 13, 3876

Organ-targeted drug delivery systems (OTDDS) of poly[(*N*-acryloylglycine)-*co*-(*N*-acryloyl-L-phenylalanine methyl ester)] copolymer library and effective treatment of triple-negative breast cancer†

Sukanya Patra,[a] Jyotirmayee,[b] Krishan Kumar,[c] Divya Pareek,[a] Prem Shankar Gupta,[a] Anjali Ramsabad Mourya,[a] Taniya Das,[a] Kirti Wasnik,[a] Malkhey Verma,[b] Ruchi Chawla,[c] Tarun Batra[d] and Pradip Paik *[a]

Organ-targeted drug delivery systems (OTDDS) are essential for the effective treatment of complicated diseases. Triple-negative breast cancer (TNBC) is an aggressive cancer with high mortality and requires targeted therapeutics. This work was aimed at designing a library of polymeric OTDDS with *N*-acryloylglycine (NAG) and *N*-acryloyl-L-phenylalanine methyl ester (NAPA) [p(NAG-*co*-NAPA)$_{(x:y)}$] and screening its *in vivo* organ-targeting specificity. Among this library, the best p(NAG-*co*-NAPA)$_{(x:y)}$ NPs with an $x:y$ ratio of 1 : 4 and size of 160–210 nm targeted breasts to a high extent compared to other organs and thus were optimized for TNBC treatment. A network pharmacology study was performed, which revealed that 14 genes were responsible for TNBC, and a combination of DHA (targets 6 genes) and piperine (targets 8 genes) drugs was used to optimize the formulation, achieving the maximum therapeutic efficiency against TNBC with an IC_{50} value of 350 μg mL^{-1}. The designed organ-specific polymeric nanoparticle (NP) library, identification of target genes and proteins responsible for TNBC, and the optimized formulation for effective combination therapy established an effective therapeutic option for TNBC. The findings of this work further demonstrate that this polymeric library of NPs shows exciting therapeutic potential for treating TNBC and presents innovative treatment options for critical diseases of the liver, heart, lungs and kidney.

Received 30th October 2024,
Accepted 12th February 2025

DOI: 10.1039/d4tb02445a

rsc.li/materials-b

1. Introduction

The precise organ-specific delivery of therapeutic biomolecules requires interdisciplinary research among scientists in chemistry and biology, engineers, and clinicians for successful treatment outcomes, given that the surface chemistry of organs is very complicated.[1] The development of effective organ-targeted drug delivery systems (OTDDS) necessitates a clear understanding of how the physical and chemical properties of OTDDS influence biological processes at the molecular, cellular and organ levels. OTDDS can deliver precise drug doses for the desired therapeutic outcomes rather than delivering an arbitrary amount of free drug at the targeted site.[2] However, for effective treatment, OTDDS must overcome challenges such as poor biodistribution and biological fate.[1] Generally, three targeting mechanisms, *i.e.*, passive, active, and endogenous, are considered to engineer OTDDS.[3–5] The passive and active targeting mechanisms have been widely studied to date. Alternatively, endogenous targeting is emerging as a promising approach based on how the chemical versatility of nanoparticles (NPs) leads to binding with distinct plasma protein subsets of target organs, directing NPs to specified organs and enhancing their cellular uptake.[6,7] However, for specific cellular uptake, controlled chemical modification of NPs is necessary. For instance, 7C1, an oligomer derived from lipidated PEI_{600}, was used for gene silencing in lung epithelial cells, compared to kidney and heart endothelial cells. However, the standardization of the lipidation process is necessary for improved silencing across different organs.[8,9] IDD-3, a terpolymer formulated with lipid components, enables

[a] School of Biomedical Engineering, Indian Institute of Technology, (Banaras Hindu University), Varanasi, Uttar Pradesh, 221 005, India. E-mail: paik.bme@iitbhu.ac.in
[b] School of Biotechnology, Institute of Science, (Banaras Hindu University), Varanasi, Uttar Pradesh, 221 005, India
[c] Department of Pharmaceutical Engineering and Technology, Indian Institute of Technology (Banaras Hindu University), Varanasi, Uttar Pradesh, 221 005, India
[d] Department of Oncology, Institute of Medical Sciences (IMS), Banaras Hindu University, Varanasi, Uttar Pradesh, 221 005, India

† Electronic supplementary information (ESI) available. See DOI: https://doi.org/10.1039/d4tb02445a

ACS Infectious Diseases

pubs.acs.org/journal/aidcbc

Review

Progress in Treatment and Diagnostics of Infectious Disease with Polymers

Sukanya Patra, Divya Pareek, Prem Shankar Gupta, Kirti Wasnik, Gurmeet Singh, Desh Deepak Yadav, Yitzhak Mastai, and Pradip Paik*

Cite This: *ACS Infect. Dis.* 2024, 10, 287−316

Read Online

ACCESS | Metrics & More | Article Recommendations

ABSTRACT: In this era of advanced technology and innovation, infectious diseases still cause significant morbidity and mortality, which need to be addressed. Despite overwhelming success in the development of vaccines, transmittable diseases such as tuberculosis and AIDS remain unprotected, and the treatment is challenging due to frequent mutations of the pathogens. Formulations of new or existing drugs with polymeric materials have been explored as a promising new approach. Variations in shape, size, surface charge, internal morphology, and functionalization position polymer particles as a revolutionary material in healthcare. Here, an overview is provided of major diseases along with statistics on infection and death rates, focusing on polymer-based treatments and modes of action. Key issues are discussed in this review pertaining to current challenges and future perspectives.

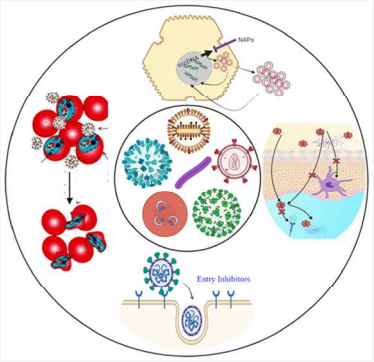

KEYWORDS: *Polymer nanoparticles, Infectious diseases, Diagnostics, Vaccination, Therapeutics*

1. INTRODUCTION

Infections play a major role worldwide contributing to ∼15% of annual death according to the World Health Organization (WHO)[1] with high mortality due to communicable diseases such as AIDS caused by human immunodeficiency virus (HIV), malaria, COVID-19 and tuberculosis (TB). Due to lack of resources, the death rates are higher in developing countries.[2] Infectious diseases are not deadly in nature. The major factors that help to spread them may be classified as economic, sociological, and/or environmental. Minor factors include changing ecosystems, poverty, famine, modern lifestyle, war, poor education, and gender inequality.[3]

Infections are caused by various pathogens including viruses, bacteria, and parasites. Viruses and parasites, although not generally considered as living, affect life considerably in this sphere. Some pathogens are surprisingly simple, while others are very complex.[4] Pathogens differ in structure, shape, replication, and interaction mechanism (Figure 1). Multiple drugs were developed and are vigorously used albeit with toxic effects and developed resistance. The overall mortality is slowly decreasing with a socio-economic gap between countries.[2] Clinical and preclinical trials lag far behind other ailments such as cancer and heart failure.[5,6]

Due to emergent multidrug-resistant pathogens and prolonged reach, topical and vector-borne diseases require a sequence of tasks. Microbiologists are fascinated by the development of diagnostics, vaccination, and prophylactic therapeutics for a wide variety of human pathogens. Polymers

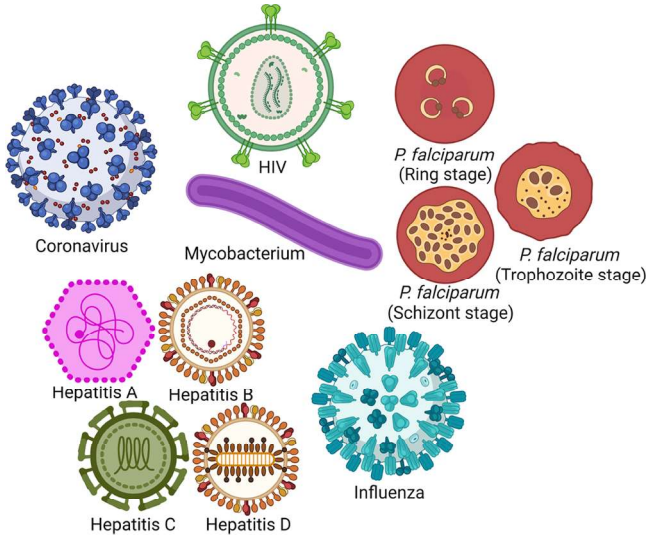

Figure 1. Viral, bacterial, and parasitic agents that underly important infectious diseases.

Received: October 2, 2023
Revised: December 19, 2023
Accepted: December 20, 2023
Published: January 18, 2024

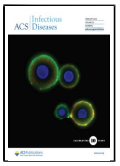

https://doi.org/10.1021/acsinfecdis.3c00528
ACS Infect. Dis. 2024, 10, 287−316

ACS APPLIED BIO MATERIALS

www.acsabm.org Review

Polymeric Nanoparticle Based Diagnosis and Nanomedicine for Treatment and Development of Vaccines for Cerebral Malaria: A Review on Recent Advancement

Sukanya Patra, Monika Singh, Kirti Wasnik, Divya Pareek, Prem Shankar Gupta, Sudip Mukherjee, and Pradip Paik*

Cite This: ACS Appl. Bio Mater. 2021, 4, 7342−7365 Read Online

ACCESS | Metrics & More | Article Recommendations

ABSTRACT: Cerebral malaria occurs due to *Plasmodium falciparum* infection, which causes 228 million infections and 450,000 deaths worldwide every year. African people are mostly affected with nearly 91% cases, of which 86% are pregnant women and infants. India and Brazil are the other two countries severely suffering from malaria endemicity. Commonly used drugs have severe side effects, and unfortunately no suitable vaccine is available in the market today. In this line, this review is focused on polymeric nanomaterials and nanocapsules that can be used for the development of effective diagnostic strategies, nanomedicines, and vaccines in the management of cerebral malaria. Further, this review will help scientists and medical professionals by updating the status on the development stages of polymeric nanoparticle based diagnostics, nanomedicines, and vaccines and strategies to eradicate cerebral malaria. In addition to this, the predominant focus of this review is antimalarial agents based on polymer nanomedicines that are currently in the preclinical and clinical trial stages, and potential developments are suggested as well. This review further will have an important social and commercial impact worldwide for the development of polymeric nanomedicines and strategies for the treatment of cerebral malaria.

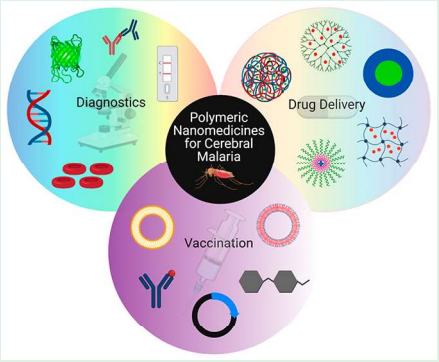

KEYWORDS: *polymeric nanomedicine, cerebral malaria, diagnostic tool, therapeutics, vaccination, clinical trials*

1. INTRODUCTION

Cerebral malaria is a notorious and malignant parasitic disease that has caused a major percentage of morbidity. According to the World Health Organization (WHO), it causes ∼228 million new infections and almost 450,000 deaths worldwide per year.[1−4] Although huge numbers of strategies and approaches have been taken into consideration to combat it, today it remains a global health burden[5−7] (Figure 1). Malaria is caused by the transmission of *Plasmodium* species, *Plasmodium vivax* (most common), *Plasmodium falciparum* (most lethal species), *Plasmodium malariae* (less harmful), and *Plasmodium ovale*,[8] which belongs to the Apicomplexa phylum.[9] According to WHO, people in developing countries including Africa and India are primarily suffering from malaria endemicity and are most vulnerable to this disease with nearly 91% cases, of which 86% are pregnant women and children below the age of 5 years.[10,11] The rate of mortality due to *P. vivax* is lower compared to that from *P. falciparum*, and it has huge socioeconomic impact in countries like Papua New Guinea, Asia, South Africa, and Oceania.[12] On the other hand, the diversity of the parasitic genome varies noticeably among various regions.[13] Genome wide association studies (GWAS) demonstrated that genetic heterogeneity is directly associated with geography and malaria parasites can be clustered depending upon continental population (partition in parasites from Asia, Africa, Cambodia, Thai-Cambodia, Thailand, and America).[14] In malaria endemic regions, for a pregnant woman, the total cost associated with malaria prognosis and therapeutics varies widely from $3.2 USD to $54 USD.[15,16] In central India it varies from $19 USD to $35 USD per household.[17] Unfortunately, malaria is still counted as a neglected disease with few therapeutic options and formulations, and no vaccines are available in the market.

The huge mortality is due to the intricate life cycle of the malaria parasite as shown in Figure 2. *Plasmodium* parasites have an intrinsic circadian clock by which they are able to synchronize to the periodic fluctuation in body temperature.[19] The infection starts through biting by a female *Anopheles* mosquito with injection of *Plasmodium* parasites into the blood

Received: May 30, 2021
Accepted: August 30, 2021
Published: September 15, 2021

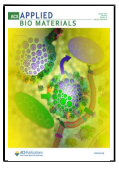

https://doi.org/10.1021/acsabm.1c00635
ACS Appl. Bio Mater. 2021, 4, 7342−7365

34% Overall Similarity

The combined total of all matches, including overlapping sources, for each database.

Match Groups

- **958** Not Cited or Quoted 33%
  Matches with neither in-text citation nor quotation marks
- **22** Missing Quotations 1%
  Matches that are still very similar to source material
- **3** Missing Citation 0%
  Matches that have quotation marks, but no in-text citation
- **0** Cited and Quoted 0%
  Matches with in-text citation present, but no quotation marks

Top Sources

7% Internet sources
32% Publications
3% Submitted works (Student Papers)

Integrity Flags

1 Integrity Flag for Review

Replaced Characters
251 suspect characters on 54 pages
Letters are swapped with similar characters from another alphabet.

Our system's algorithms look deeply at a document for any inconsistencies that would set it apart from a normal submission. If we notice something strange, we flag it for you to review.

A Flag is not necessarily an indicator of a problem. However, we'd recommend you focus your attention there for further review.

Match Groups

- 958 Not Cited or Quoted 33%
  Matches with neither in-text citation nor quotation marks
- 22 Missing Quotations 1%
  Matches that are still very similar to source material
- 3 Missing Citation 0%
  Matches that have quotation marks, but no in-text citation
- 0 Cited and Quoted 0%
  Matches with in-text citation present, but no quotation marks

Top Sources

- 7% Internet sources
- 32% Publications
- 3% Submitted works (Student Papers)

Top Sources

The sources with the highest number of matches within the submission. Overlapping sources will not be displayed.

1	Publication	
Pradip Paik, Sukanya Patra, Jyotirmayee Jyotirmayee, Krishan Kumar et al. "Orga...		21%
2	Publication	
Sukanya Patra, Jyotirmayee, Krishan Kumar, Divya Pareek et al. " Organ-targeted...		3%
3	Publication	
Premshankar Gupta, Kirti Wasnik, Sukanya Patra, Divya Pareek, Gurmeet Singh, ...		<1%
4	Student papers	
Banaras Hindu University		<1%
5	Publication	
Sukanya Patra, Monika Singh, Divya Pareek, Kirti Wasnik, Prem S. Gupta, Pradip P...		<1%
6	Internet	
www.ncbi.nlm.nih.gov		<1%
7	Publication	
Prem Shankar Gupta, Kirti Wasnik, Gurmeet Singh, Sukanya Patra et al. " potenti...		<1%
8	Internet	
www.frontiersin.org		<1%
9	Internet	
www.researchgate.net		<1%
10	Internet	
rua.ua.es		<1%

11	Publication	
Dong-Hee Choi, Hui-wen Liu, Yong Hun Jung, Jinchul Ahn et al. "Analyzing angiog...		<1%
12	Publication	
Prem Shankar Gupta, Kirti Wasnik, Sukanya Patra, Divya Pareek, Gurmeet Singh, ...		<1%
13	Internet	
www.science.gov		<1%
14	Publication	
Pradip Paik, Kirti Wasnik, Premshankar Gupta, Gurmeet Singh et al. "Neurogenic ...		<1%
15	Publication	
Divya Pareek, MD Zeyalluah, Sukanya Patra, Oviya Alagu, Gurmeet Singh, Kirti W...		<1%
16	Internet	
www.mdpi.com		<1%
17	Internet	
worldwidescience.org		<1%
18	Internet	
www.nature.com		<1%
19	Publication	
Rajalaxmi Pradhan, Subarno Paul, Biswajit Das, Saptarshi Sinha, Somya Ranjan D...		<1%
20	Publication	
Roxana E. Oberkersch, Massimo M. Santoro. "Role of amino acid metabolism in a...		<1%
21	Internet	
pubs.rsc.org		<1%
22	Publication	
Anil Kumar Yamala, Vinod Nadella, Yitzhak Mastai, Hridayesh Prakash, Pradip Pai...		<1%
23	Publication	
Mohammed Gulzar Ahmed, Sumel Ashique, Arshad Farid, Gokhan Zengin. "Nano...		<1%
24	Internet	
iv.iiarjournals.org		<1%

25 Internet
www.sabcs.org <1%

26 Publication
Yan Xu, Xiangmei Jin, Jun Zhang, Kun Wang, Xiaoyan Jin, Dongyuan Xu, Xizhe Tian... <1%

27 Internet
mdpi-res.com <1%

28 Internet
scholarscompass.vcu.edu <1%

29 Internet
patents.justia.com <1%

30 Publication
Rajapakse, Rajapakse Arachchige Dhanusha Nayanangani. "Investigation of Co-A... <1%

31 Internet
link.springer.com <1%

32 Internet
www.tandfonline.com <1%

33 Student papers
J S S University <1%

34 Publication
Shixian Lv, Zhaohui Tang, Mingqiang Li, Jian Lin, Wantong Song, Huaiyu Liu, Yubi... <1%

35 Internet
www.karger.com <1%

36 Publication
"Poster Presentations", FEBS Journal, 2012. <1%

37 Publication
Afrin, Sadia. "Eugenol Loaded Calcium Citrate Particle as a pH Triggered Drug Rel... <1%

38 Publication
Kirti Wasnik, Gurmeet Singh, Desh Deepak Yadav, Sukanya Patra et al. " Poly[(-ac... <1%

39 Internet
archive-ouverte.unige.ch <1%

40 Internet
pubs.acs.org <1%

41 Internet
www.rsc.org <1%

42 Publication
Kirti Wasnik, Prem Shankar Gupta, Sudip Mukherjee, Alagu Oviya et al. " Poly(-ac... <1%

43 Internet
nagoya.repo.nii.ac.jp <1%

44 Publication
Premshankar Gupta, Kirti Wasnik, Gurmeet Singh, Sukanya Patra et al. "In vivo P... <1%

45 Internet
gnosis.library.ucy.ac.cy <1%

46 Internet
www.connectpos.com <1%

47 Publication
Timothy P. Lodge, Paul C. Hiemenz. "Polymer Chemistry", CRC Press, 2020 <1%

48 Publication
Y. Yagci, M.K. Mishra, O. Nuyken, K. Ito, G. Wnek. "Tailored Polymers & Applicatio... <1%

49 Internet
bmccancer.biomedcentral.com <1%

50 Internet
ir.amu.ac.in <1%

51 Internet
www.bmva.org <1%

52 Publication
Chad A. Mirkin. "Spherical Nucleic Acids", Jenny Stanford Publishing, 2021 <1%

53	Publication	
Hideharu Mori, Takeshi Endo. "Amino-Acid-Based Block Copolymers by RAFT Poly...		<1%
54	Publication	
Kirti Wasnik, Prem Shankar Gupta, Gurmeet Singh, Somedutta Maity et al. " Neur...		<1%
55	Internet	
www.ccspublishing.org.cn		<1%
56	Internet	
d-nb.info		<1%
57	Internet	
ubir.buffalo.edu		<1%
58	Internet	
www.freepatentsonline.com		<1%
59	Internet	
www.thno.org		<1%
60	Publication	
Hideharu Mori, Eri Takahashi, Ai Ishizuki, Kazuhiro Nakabayashi. "Tryptophan-Co...		<1%
61	Internet	
patents.glgoo.top		<1%
62	Internet	
www.ros.hw.ac.uk		<1%
63	Publication	
Adinew, Getinet M.. "Thymoquinone Anticancer Effects through Cell Cycle Arrest, ...		<1%
64	Publication	
Sudhakar Behera, Rakesh Kumar Gautam, Sunil Mohan, Arghya Chattopadhyay. "...		<1%
65	Internet	
dspace.nwu.ac.za		<1%
66	Internet	
iris.unimore.it		<1%

67 Internet
pmc.ncbi.nlm.nih.gov <1%

68 Internet
www.bio-nica.info <1%

69 Publication
Singh, Nirupama. "Synthesis of Poly(L-Glutamine) of Controlled Chain Length: A N... <1%

70 Internet
gyan.iitg.ernet.in <1%

71 Publication
Kirti Wasnik, Gurmeet Singh, DESH DEEPAK Deepak YADAV, Divya Pareek et al. "P... <1%

72 Publication
Leopoldo Javier Ríos González, Jośe Antonio Rodríguez-De La Garza, Miguel Ángel ... <1%

73 Publication
Mu Zhang, Lei Wan, Ruiqi Li, Xiaoling Li, Taifu Zhu, Haibin Lu. "Engineered exoso... <1%

74 Student papers
TAFE Queensland Brisbane <1%

75 Student papers
University of Hong Kong <1%

76 Student papers
Vel Tech University <1%

77 Internet
centaur.reading.ac.uk <1%

78 Internet
ebin.pub <1%

79 Internet
phys.org <1%

80 Student papers
Imperial College of Science, Technology and Medicine <1%